Facies (2014) 60:347–369
DOI 10.1007/s10347-013-0370-4

ORIGINAL ARTICLE

Facies development and sequence stratigraphy of the Ludfordian (Upper Silurian) deposits in the Zbruch River Valley, Podolia, western Ukraine: local facies overprint on the $\delta^{13}C_{carb}$ record of a global stable carbon isotope excursion

Emilia Jarochowska · Wojciech Kozłowski

Received: 18 December 2012 / Accepted: 11 April 2013 / Published online: 3 May 2013

Abstract The Ludfordian (Upper Silurian) succession in Podolia, western Ukraine, represents a Silurian carbonate platform developed in an epicontinental sea on the shelf of the paleocontinent of Baltica. Coeval deposits throughout this basin record a positive stable carbon isotope excursion known as the Lau excursion. The record of this excursion in Podolia exhibits an unusual amplitude from highly positive (+6.9 ‰) to highly negative (−5.0 ‰) $\delta^{13}C_{carb}$ values. In order to link $\delta^{13}C_{carb}$ development with facies, five sections in the Zbruch River Valley were examined, providing microfacies characterization and revised definitions of the Isakivtsy, Prygorodok, and Varnytsya Formations. The Isakivtsy Fm. is developed as dolosparite replacing originally bioclastic limestone. The Prygorodok Fm., recording strongly depleted (down to −10.53 ‰) to near zero (0.12 ‰) $\delta^{13}C_{carb}$ values is developed as laminated, organic-rich dolomicrite with metabentonite and quartz siltstone beds. The Varnytsya Fm. is characterized by peritidal deposition with consistent, slightly negative $\delta^{13}C_{carb}$ values (−0.57 to −3.20 ‰). It is proposed that dolomitization of the Isakivtsy Fm. is associated with a sequence boundary and erosional surface. The overlying Prygorodok Fm. represents the proximal part of a TST deposited in restricted and laterally extremely variable environments dominated by microbial carbonate production. The transition to the overlying Varnytsya Fm. facies is marked by a maximum flooding surface. The SB and MFS are potentially correlative within the basin and support a global rapid sea-level fall previously proposed for this interval. The interpretation of the Prygorodok Fm. as coastal lake deposits may explain the unusual $\delta^{13}C_{carb}$ values and constitute one of the few records of this type of environment identified in the early Paleozoic.

Keywords Lau Event · Baltica · Lacustrine environments · Microbial dolomite precipitation · Stable carbon isotopes

Introduction

The Ludfordian (Upper Silurian) stage was the time of the most pronounced positive stable carbon isotope excursion (CIE) in the Phanerozoic, known as the Lau excursion (Wenzel and Joachimski 1996; Bickert et al. 1997; Wigforss-Lange 1999; Calner et al. 2004; Martma et al. 2005; Kaljo and Martma 2006; Jeppsson et al. 2007; Kaljo et al. 2007; Lehnert et al. 2007; Eriksson and Calner 2008; Barrick et al. 2010; Kozłowski and Munnecke 2010; Munnecke et al. 2010; Cramer et al. 2011; Loydell and Frýda 2011; Jeppsson et al. 2012; Kaljo et al. 2012; Kozłowski and Sobień 2012). Very good geochemical, biostratigraphical, and paleoecological documentation exists for the Lau excursion, and it is often used as a model to study positive CIEs, which are widely used as chemostratigraphic markers and as indicators of perturbations of the global carbon cycle (Jeppsson 1990; Aldridge et al.

Electronic supplementary material The online version of this article (doi:10.1007/s10347-013-0370-4) contains supplementary material, which is available to authorized users.

E. Jarochowska · W. Kozłowski
Institute of Geology, University of Warsaw, Al. Żwirki i Wigury 93, 02-089 Warsaw, Poland
e-mail: woko@uw.edu.pl

Present Address:
E. Jarochowska (✉)
GeoZentrum Nordbayern, Fachgruppe Paläoumwelt, Loewenichstr. 28, 91054 Erlangen, Germany
e-mail: emilia.jarochowska@gzn.uni-erlangen.de

1993; Bickert et al. 1997; Jeppsson and Aldridge 2000; Munnecke et al. 2003; Calner 2005a; Melchin and Holmden 2006; Cramer and Saltzman 2007a, b; Fanton and Holmden 2007; Calner et al. 2008; Małkowski et al. 2009; Kozłowski and Sobień 2012). Studies of recent and sub-fossil carbonate sediments indicate that sea-level forcing, restricted circulation and laterally variable sediment composition can significantly influence the $\delta^{13}C_{carb}$ values, leading to amplification of positive excursions in carbonate platform interiors during flooding intervals (Immenhauser et al. 2003; Swart and Eberli 2005; Swart 2008; Gischler et al. 2009; Oehlert et al. 2012). The small-scale spatial variability of $\delta^{13}C$ values results from a combination of generic marine-water signal and local factors such as facies, restricted circulation, and diagenetic overprint. Although it is difficult to attribute the final $\delta^{13}C$ values to the influence of a particular factor, in some cases it can be demonstrated (e.g., Holmden et al. 1998; Harzhauser et al. 2007; Colombié et al. 2011). Some local factors seem to have been involved in the record of the Lau excursion, which is mostly documented by $\delta^{13}C_{carb}$ of limestones from the epicontinental basin developed during the early Paleozoic on Baltica. This Ludfordian CIE has been recorded in Sweden (+11.2 ‰, Wigforss-Lange 1999; +8.80 ‰, Samtleben et al. 2000), Lithuania (+8.2 ‰, Martma et al. 2005), Latvia (+5 ‰, Kaljo and Martma 2006; Kaljo et al. 2012), Poland (+8.9 ‰, Kozłowski and Munnecke 2010; +6.7 ‰, Kozłowski and Sobień 2012) and Ukraine (+6.9 ‰, Kaljo et al. 2007; +6.0 ‰, Kaljo et al. 2012). These localities represent different settings across the carbonate platform and enable the detection of local variability in the CIE record and its dependence on local facies development. Kaljo et al. (2012) reported substantial differences in the record of the Ludfordian CIE in closely spaced shallow-water sections located in the Podolia region of western Ukraine, including strongly depleted values (down to −5.0 ‰) within or slightly above the positive peak. In the present paper, five lithological sections in the Zbruch River Valley in Podolia, representing the Lau excursion interval, have been investigated. We provide a detailed microfacies analysis, review, and update descriptions of lithostratigraphic units, identify their sequence stratigraphic positions and their potential correlation with depositional sequences reported from other sections within and outside the basin. An explanation is proposed for the unusual $\delta^{13}C_{carb}$ values occurring in this interval in the Zbruch River valley and elsewhere in Podolia.

Materials and methods

Sections investigated in the present study are exposed along the lower reaches of the Zbruch River, ca. 8 km upstream of its outlet into Dniester, and the stretch between the villages of Chernokozyntsi and Zavalya (Fig. 1). Outcrops are located on both banks of the Zbruch River in deeply incised slopes. In view of the lack of detailed topographical maps of the area, localization of the outcrops was primarily based on satellite photographs and GPS coordinates (given in the supplementary online material 1). The sections Kudryntsi–Castle and Kudryntsi–Cowpath have been additionally correlated using a dumpy level and the results have been integrated in the final correlation chart (Fig. 2, with a larger version in the supplementary online material 2).

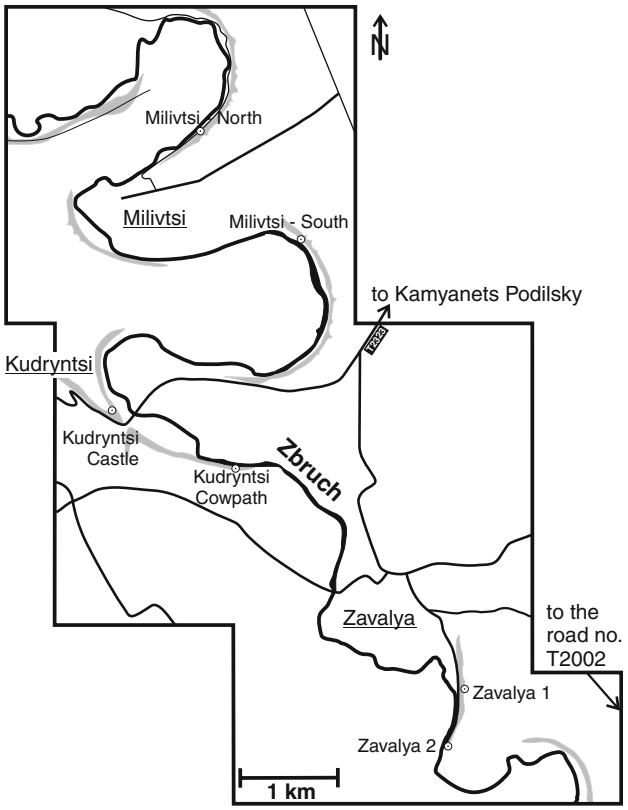

Fig. 1 Map of the study area: the lower reaches of the Zbruch River, south of the city of Skala Podilska with positions of described sections. *Grey areas* indicate continuous belts of Silurian outcrops in the river valley slopes

For stable carbon isotope measurements of carbonates, 16 unweathered samples and two brachiopods were selected. Vein-free pelitic matrix and unaltered shell fragments were powdered using a steel needle and analyzed in the Stable Isotope Laboratory of the Polish Academy of Sciences in Warsaw. Sample powder was treated with phosphoric acid in a Kiel IV preparation system and analyzed in a conjunct Finnigan Delta + mass spectrometer. Values are reported in Table 1 using the conventional delta notation with respect to the Vienna Pee Dee Belemnite (VPDB). Reproducibility for the isotopic analysis was better than ±0.1 %.

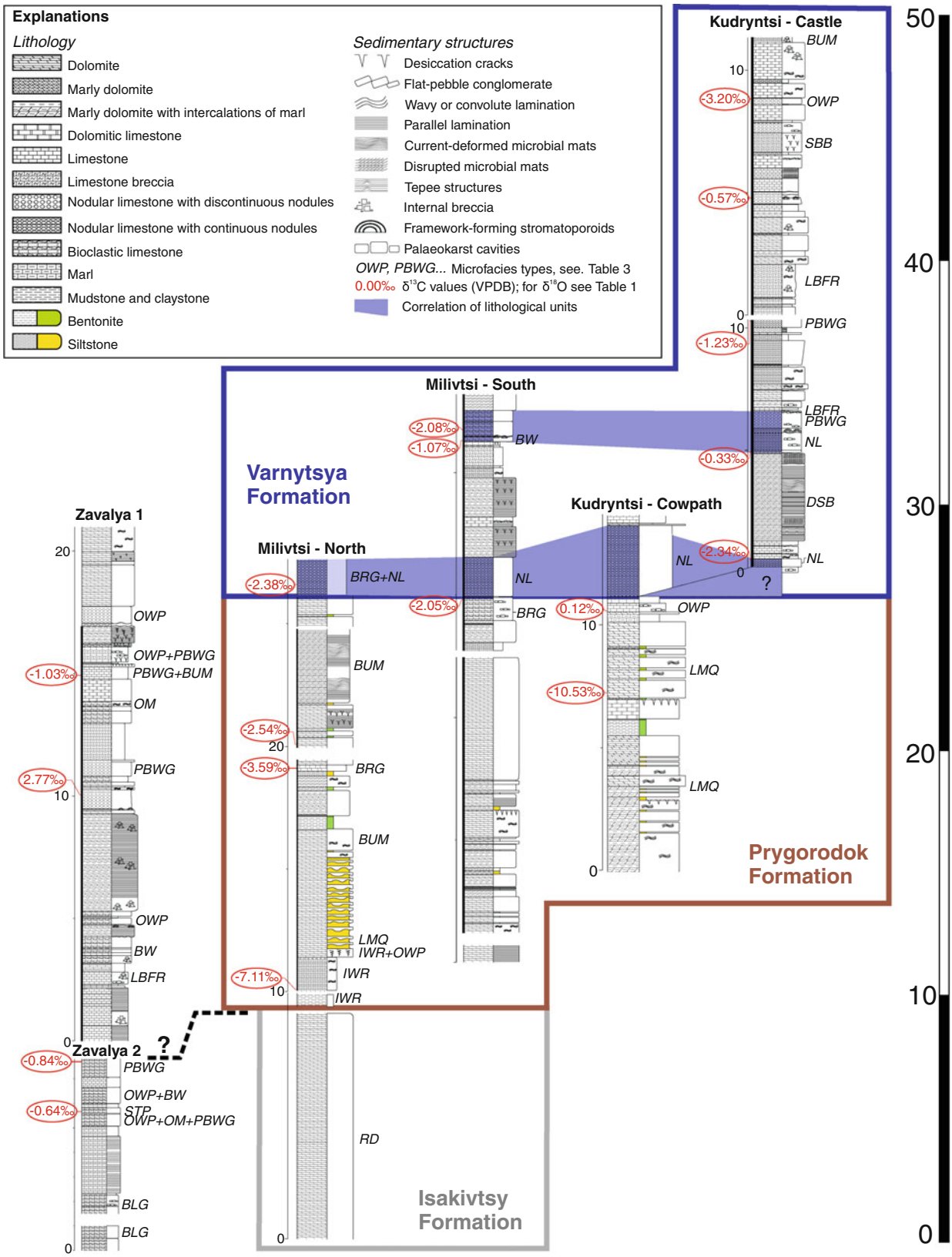

Fig. 2 Correlation of sections based on lithology, topographic position, and dumpy leveling, with an assignment to lithostratigraphic units discussed in the text

Table 1 Stable carbon and oxygen isotope ratios (VPDB)

Sample	$\delta^{13}C_{carb}$	$\delta^{18}O$
Zavalya2 7	−0.64	−6.53
Zavalya2 11	−0.84	−7.50
Zavalya1 22[a]	2.77	0.58
Zavalya1 33	−1.03	−5.35
Milivtsi N 2	−7.11	−3.63
Milivtsi N 7	−3.59	−6.53
Milivtsi N 8	−2.54	−2.95
Milivtsi N 18A	−2.38	−5.96
Milivtsi S 36	−2.05	−7.45
Milivtsi S 45	−1.07	−6.64
Milivtsi S 46	−2.08	−7.52
Cowpath 10	−10.53	−5.27
Cowpath 15	0.12	−4.99
CastleL 3	−2.34	−7.18
CastleL 11[a]	−0.33	−6.09
CastleL 22	−1.23	−6.21
CastleU 15.2	−0.57	−7.33
CastleU 26	−3.20	−6.38

Sample positions are marked on lithological sections

[a] Values from brachiopod shells

Study area

Silurian outcrops in the region of Podolia, western Ukraine, expose the sedimentary rocks deposited on the south-western shelf of Baltica in a basin that stretched from present-day southern Sweden through to Moldova (Fig. 3). Surface exposures in Podolia represent shallow-water carbonate facies developed on a vast epeiric platform, which extended basinward into the shelf facies recognized today in the subsurface of Poland (Teller 1997; Kozłowski and Sobień 2012), Baltic countries (Kaljo 1970; Kaljo et al. 1997; Martma et al. 2005), as well as in Sweden (Samtleben et al. 2000; Calner et al. 2006).

Geological context

Lithostratigraphy

Two main lithostratigraphical schemes exist for the Silurian of Podolia: one developed by the research group of Nikiforova (Nikiforova and Predtechenskij 1968; Nikiforova et al. 1972), and the second by Tsegelnyuk (Tsegelnyuk 1980a, 1980b) and Tsegelnyuk et al. (1983). Herein the latter scheme is followed, as it corresponds more closely with our own observations on the facies development within the studied interval. Tsegelnyuk et al. (1983) distinguished four main "series" in the Silurian of Podolia: Bolotyn, Yaruga, Malinovtsy, and Rukshin, and related them, respectively, to the Llandovery, Wenlock, Ludlow, and Downton series of the Anglo-Welsh Basin.

The outcrop belt of the Malinovtsy Series is spread between the villages of Bolshaya Slobodka to Isakivtsy. It reaches a thickness of 90–141 m and is subdivided into three suites: the Konovka, Tsviklivtsy, and Rykhta suites. Of particular interest for the present study is the Rykhta suite, which is divided into the Grinchuk sub-suite, represented by marly nodular limestone and marlstone, and the overlying Isakivtsy sub-suite, represented by dolomitized grainstone with remains of a diverse fauna, including tabulate corals, stromatoporoids, algae, crinoids, gastropods, and brachiopods. The sub-suites of Grinchuk and Isakivtsy reach thicknesses of 18–19 and 5–6 m, respectively.

The lower boundary of the Rukshin series is drawn at the base of a black shale or marly dolomite of the Prygorodok suite that rest on an erosion surface at the top of the dolomite of the Isakivtsy sub-suite. The total thickness of the Rukshin series reaches 250 m in the outcrop belt from Khotin to Melnytsya-Podilska. Of the five suites of the Rukshin series, namely Prygorodok, Varnytsya, Trubchyn, Dzvenygorod, and Khudykivtsy, the first two are relevant to the interval studied in the present work. An additional help in local correlation is the presence of six K-bentonite beds numbered C1–C6 in the Prygorodok suite, and two more (C7, C8) in the Varnytsya suite, characterized geochemically by Huff et al. (2000) and Kiipli et al. (2000).

Abushik et al. (1985) have reintroduced the term "Skala series", originally employed by Alth (1874), and described the Skala Series deposits in the Zbruch River Valley. Abushik et al. (1985) distinguished only two "formations" (used interchangeably with "suites") within the Skala series: Rashkov and Dzvenygorod. The lower boundary of the Skala Series was placed by these authors at the abrupt lithological change from argillaceous dolomite devoid of fossils, which is attributed to the upper sub-suite of the Isakivtsy suite, to the shallow-marine deposits associated with the Rashkov suite. Based on lithological profiles of key sections employed to characterize these units, it can be inferred that the Isakivtsy Formation sensu Abushik et al. (1985) and Koren' et al. (Koren' et al. 1989) includes the Isakivtsy sub-suite and the Prygorodok suite of Tsegelnyuk et al. (1983) in the rank of sub-suites (Table 2). The Rashkov suite was distinguished on the basis of depositional cycles, which are identified in the present study as peritidal. As the Skala Series has been subsequently used to denote Přídolí in the regional stratigraphic scheme for Podolia (Koren' et al. 1989), this unit is adopted here as a synonym for the Rukshin Series defined by Tsegelnyuk et al. (1983).

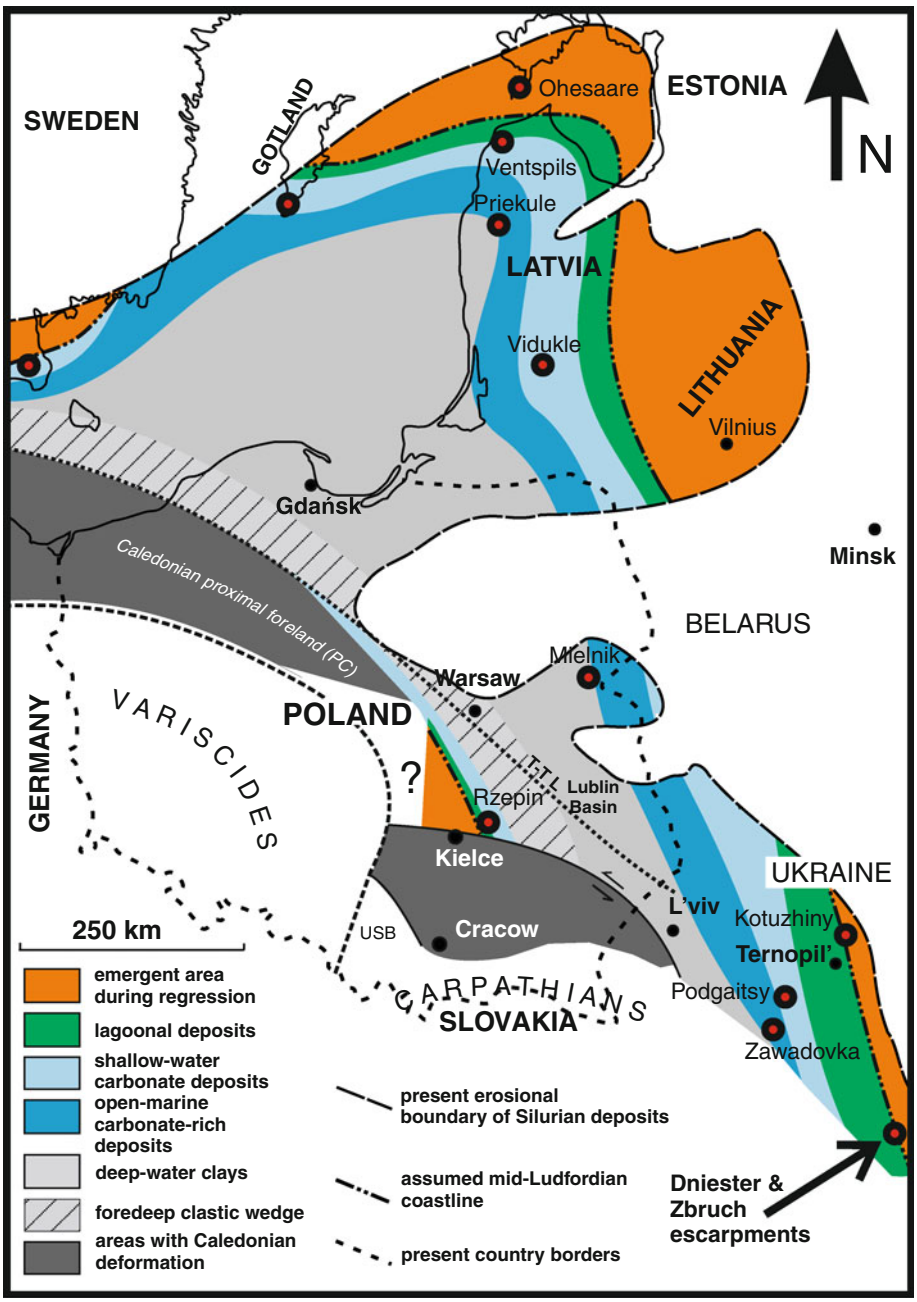

Fig. 3 Paleogeographic map of the study area and its position on the SW shelf of Baltica in the Upper Ludfordian, based on Einasto et al. (1986) and Teller (1997). *USB* Upper Silesian Block, *PC* Pomeranian Caledonides, *T-TL* Teisseyre-Tornquist Line, *red dots* coring localities and sections mentioned in the text, *black dots* present-day cities

Biostratigraphy

In the standard regional scheme for the Silurian of Podolia by Koren' et al. (Koren' et al. 1989) counterparts of the Isakivtsy and Prygorodok Fms are placed entirely in the Ludfordian Stage, and the boundary between the Prygorodok Fm. and the Varnytsya Fm. is placed at the Ludlow-Přídolí boundary. Abushik et al. (1985) reported occurrences of *Ozarkodina crispa* in the lower member of the Rashkov suite, corresponding to the Varnytsya Fm., which indicates its Ludfordian age. These authors reported the *O. eosteinhornensis* assemblage from the middle Rashkov sub-suite, corresponding to the upper part of the Varnytsya Fm. and establishing its Přídolí age. However, Paris and Grahn (1996) reported *Eisenackitina barrandei* in the Dzvenygorod Formation, suggesting that the entire underlying Varnytsya Fm. is of Ludfordian age. This disagreement may result from diachronous boundaries between the Varnytsya and Dzvenigorod Fms. While the studies do not completely agree, both place the lower part of the Varnytsya Fm. in the Ludfordian Stage (see correlation of flooding surfaces in the discussion).

Table 2 Correlation between lithostratigraphical units in the Ludfordian to Přídolí of Podolia, distinguished by Abushik et al. (1985) and Tsegelnyuk et al. (1983)

Abushik et al. (1985)			Tsegelnyuk et al. (1983)
Suite	Sub-suite	Thickness (m)	
Dzvenygorod	Not distinguished	22	Dzvenygorod suite
Rashkov	Upper sub-suite	44	Trubchyn suite
	Middle sub-suite	22.5	Varnytsya suite
	Lower sub-suite	17	
Isakivtsy	Upper sub-suite	20	Prygorodok suite
	Lower sub-suite	9.3	Isakivtsy sub-suite

These findings constrain the age of the studied rocks from the top. From the bottom, it has been constrained by Paris and Grahn (1996), who identified *Sphaerochitina sphaerocephala* and *E. barrandei* in the top part of the Isakivtsy Fm. The Ludfordian age of these deposits is also supported by the presence of *Daya navicula* in the uppermost Grinchuk, Isakivtsy and Prygorodok Fms. (Tsegelnyuk et al. 1983; Nikiforova et al. 1985) and of *Homoeospira baylei* in the last two formations (Nikiforova et al. 1985).

Stable carbon isotope stratigraphy

Of potential utility for constraining the stratigraphic position of the interval investigated in the present study is the positive stable CIE recognized globally in the Ludfordian (Wenzel and Joachimski 1996; Bickert et al. 1997; Kaljo et al. 1997; Azmy et al. 1998; Wigforss-Lange 1999; Wenzel et al. 2000; Saltzman 2001; Calner 2005b; Martma et al. 2005; Kaljo and Martma 2006; Jeppsson et al. 2007; Kaljo et al. 2007; Lehnert et al. 2007; Eriksson and Calner 2008; Barrick et al. 2010; Kozłowski and Munnecke 2010; Munnecke et al. 2010; Cramer et al. 2011; Loydell and Frýda 2011; Kaljo et al. 2012; Kozłowski and Sobień 2012; Manda et al. 2012). The beginning of the excursion coincides with an abrupt decrease in abundance of *Polygnathoides siluricus*, shortly before its *Last Appearance Datum* (LAD) (Martma et al. 2005; Kaljo and Martma 2006; Jeppsson et al. 2007; Lehnert et al. 2007; Eriksson and Calner 2008). The peak interval is constrained within the *O. snajdri* zone (coeval with the top of the *Neocucullograptus kozlowskii* zone), and in many sections there is lithological evidence for a sub-stratigraphic (contained entirely within one biozone) gap or even erosion (Kaljo et al. 1997; Calner 2005b; Lehnert et al. 2007; Eriksson and Calner 2008; Kozłowski and Munnecke 2010; Loydell and Frýda 2011; Kaljo et al. 2012; Kozłowski and Sobień 2012). The position of the falling limb of the excursion is less consistent. The CIE ends clearly below the *First Appearance Datum* (FAD) of *O. crispa* in Gotland (Calner et al. 2004; Jeppsson et al. 2007; Eriksson and Calner 2008), as well as in the Ventspils (Latvia) and Vidukle-61 (Lithuania) cores (Martma et al. 2005; Kaljo and Martma 2006; Kaljo et al. 2012), but it persists over a much longer interval in the Ohesaare core (Saarema, Estonia). Data available from the Bohemian Basin (Lehnert et al. 2007) and from the Anglo-Welsh Basin (Loydell and Frýda 2011) also suggest that the return to values close to 0 ‰ predates the first appearance of *O. crispa*.

The excursion has been confirmed by Kaljo et al. (2007, 2012) in the Dniester River valley, where it begins entirely in the Prygorodok Fm. (Isakivtsy-45 locality, max. $\delta^{13}C = 6.0$ ‰) or well within the Isakivtsy Fm. (Zhvanets-39 locality, max. $\delta^{13}C = 6.6$ ‰). Under the assumption that metabentonite beds in the Prygorodok Fm. are isochrones, the return to base-level values is clearly diachronous, e.g., between the Ataki-117 + Braga-119 section (Kaljo et al. 2007; below the C2 metabentonite bed) and the Isakivtsy-45 section (Kaljo et al. 2012; below the C3 metabentonite bed). These authors also introduced the "top Ludfordian twin excursion" based on the analysis of the Vidukle-61 and Ohesaare cores, where this smaller double peak is developed entirely within the *O. crispa* zone. This separate twin peak is, however, not visible in most sections, but elevated $\delta^{13}C$ values seem to decay at various rates (Kaljo et al. 1997; Kaljo and Martma 2006; Kozłowski and Munnecke 2010; Kaljo et al. 2012). According to Kaljo et al. (2012), the Ludfordian excursion in Podolia is entirely contained within the Isakivtsy and Prygorodok Fms and the $\delta^{13}C_{carb}$ values are close to 0 ‰ in the Varnytsya Fm.

Results

Characterization of lithostratigraphic units and depositional environments

The Isakivtsy Formation

Dolomite belonging to the Isakivtsy Formation is exposed in the Zbruch River Valley along a continuous belt of

outcrops stretching from Milivtsi along the eastern bank of the Zbruch River, up to the floodplain below the village of Chernokozyntsi, where they disappear under vegetation.

Macroscopically, the Isakivtsy dolomite forms a massive unit, the top of which is clearly marked in the topography of the valley slopes (Fig. 4a). The topmost 3–6 m of the unit is formed by unbedded dolosparite with the degree of recrystallization decreasing towards the bottom of the section, where the dolomite is argillaceous and less resistant to weathering. Weathered surfaces reveal coquinas formed by brachiopods and ostracods (Fig. 4b). The total thickness of the deposits of the Isakivtsy Fm. could not be determined, but it clearly reaches more than 10 m (Fig. 2).

The Isakivtsy dolosparite, characterized in detail as microfacies RD in Table 3 and in Fig. 4c, is inequigranular and planar-subhedral (classification of Sibley and Gregg 1987, which is also used in the descriptions that follow). Cap-in-cap structures formed of disarticulated ostracod carapaces indicate that the original sediment may have been subjected to wave action. Based on these characteristics, it is proposed that the original rock was formed in a relatively restricted, but marine environment, e.g., a shallow lagoon.

The Prygorodok Formation

Deposits representing the Prygorodok Fm. reach a thickness of 17 m in the studied area (Fig. 2) and the most complete profile is accessible in the Milivtsi–North section (Fig. 4d). Auxiliary profiles are available in the Milivtsi–South (Fig. 5a) and Kudryntsi–Cowpath sections (Fig. 6a). The dominant lithology is argillaceous dolomite.

In the basal part, a breccia is present composed of angular intraclasts up to 10 cm in diameter (microfacies IWR in Table 3). The dominant clast lithology is dark brown, centimeter-scale laminated dolomicrite, argillaceous and rich in organics (Fig. 4e, g, h), which binds fine sand-sized angular quartz grains with admixtures of biotite. The process of brecciation affected sediment, which was already partly stabilized by lithified dolomitic crusts (Fig. 4i).

Microbial carbonates are present throughout the formation, forming massive dolomicrite beds with an admixture of quartz (microfacies LMQ in Table 3), or undulating, deformed sheets covered with mudcracks (Fig. 4h, i). Wrinkle structures (Fig. 5c) and load casts (Figs. 4h, 5e) indicate that lamination of the dolomite is stromatolitic, but locally affected by current action (Fig. 6c). Microbial crusts occur upon and stabilize yellow siltstone beds ranging from 1 to 15 cm in thickness, formed of unlithified quartz grains with a high carbonate content (Fig. 4i). Typically, the lower boundary of a siltstone bed is sharp, and the top undulates as it was stabilized by microbial mats. In the Milivtsi–South section there are two horizons of cube-shaped pseudomorphs, 1–5 mm in diameter (Fig. 5d).

In the upper part of the Prygorodok Fm., the proportion of laminated sediments decreases and bedding in the dolomite thickens and becomes massive in the uppermost part. The color is lighter, probably indicating a more oxygenated environment. The thick-bedded marly dolomite is poor in fossils, except for burrows (Fig. 4f, microfacies BUM in Table 3). Silicified leperditicopid ostracods are concentrated in several horizons (microfacies OWP in Table 3; Fig. 4j). The silica was likely derived from metabentonite beds, which are present in substantial thicknesses (up to tens of centimeters) and in vivid colors (Figs. 2, 5b, 6b, d, e). The Kudryntsi–Cowpath section contains a distinctive 4-cm-thick bed of laminated fine-grained volcanogenic sandstone-claystone (Fig. 6b, d, e), consisting of sub-millimeter-scale alternations of fine quartz and clay layers, which indicates sedimentation from suspension.

The massive dolomite contains several shell beds composed of normally graded shells with convex-up orientation (microfacies BRG in Table 3; Fig. 4k, m). The lower boundary of each shell bed is erosional (Fig. 4m). The crushed and reworked fauna bioclasts contain evidence of organisms not occurring in the Prygorodok Fm., such as tabulate corals and bryozoans.

On the upper bedding planes of shell beds, gastropod and bivalve shells are current-aligned. Although the shell beds represent sediment transported shoreward, the allochthonous faunal assemblage is poorly diversified, pointing to a restricted lagoonal environment as a source area for the redeposited material. These shell beds are interpreted as either tempestites or washover-fan deposits. The lateral extent of these beds could not be determined, as all examined outcrops did not exceed 5 m in width. The proportion of this type of event bed increases towards the top of the Prygorodok Fm., along with the diversity of bioclasts (qualitative observation).

Stable carbon isotope development

The laminated dolomite just above the breccia level in the Milivtsi-North outcrop has a $\delta^{13}C_{carb}$ value of −7.11 ‰ and the minimum value of −10.53 ‰ is reached within the thin-bedded laminated dolomite in the Kudryntsi–Cowpath section (the position of carbon isotope samples is indicated on the lithological profiles in Fig. 2). Above the laminated dolomite, the $\delta^{13}C_{carb}$ values in the uppermost part of the Prygorodok Fm. rise to −2.54 ‰ within the Milivtsi–North section and to −2.05 ‰ in the Milivtsi–South section just below the nodular limestone bed marking the boundary with the Varnytsya Fm.

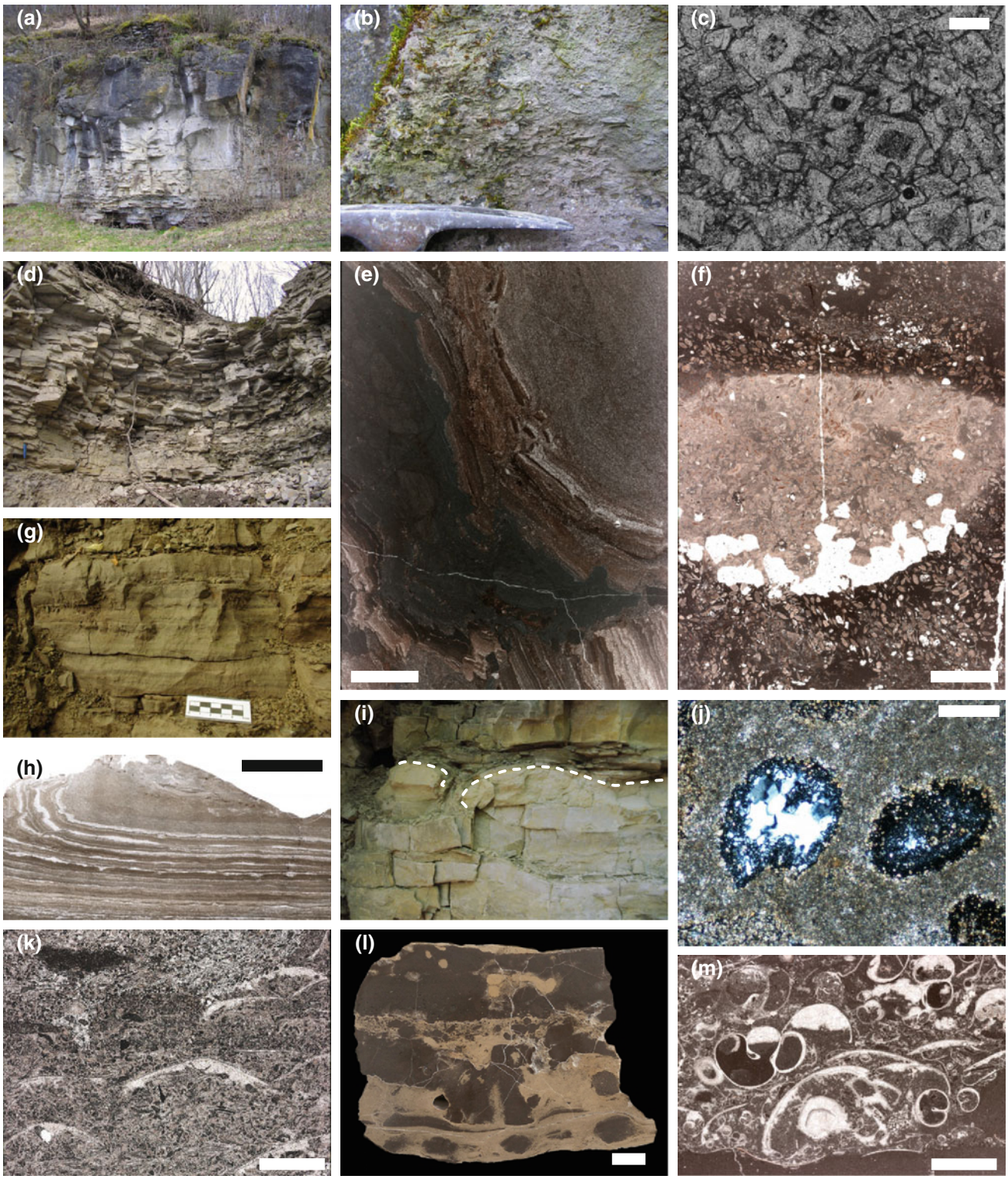

Interpretation of the environment of deposition

The proposed interpretation of the environment of deposition of the Prygorodok Fm. is a system of extremely restricted water bodies, likely cut off from open-marine waters following a drop in sea level. This interpretation is based on the following features of the studied deposits, selected from known features of carbonate lakes (summarized in Freytet and Verrecchia 2002; Gierlowski-Kordesch 2010):

◀**Fig. 4** The Milivtsi–North section. **a–c** The Isakivtsy Fm. **a** Top part of the dolomite unit. Outcrop height is approx. 7 m. The overlying deposits of the Prygorodok Fm. form a gentle slope and are usually overgrown with thick vegetation. **b** Shell accumulation on weathered surfaces of the Isakivtsy dolomite. **c** Dolomite rhombohedra in the matrix exhibit cloudy cores, which may be the remnants of the original mineralogical phase; *scale* 100 μm. **d–m** Prygorodok Fm. **d** Thick-bedded to massive silty dolomite (*hammer* for scale). **e** Brecciated laminated marly dolomite in the basal part of the Prygorodok Fm. Clasts are overturned, but remain in situ; *scale* 5 mm. **f** Cross section of a burrow within the marly dolomicrite, formed in bioturbated ostracod wackestone; *scale* 5 mm. **g** Laminated, highly argillaceous dolomicrite in the basal part of the Prygorodok Fm; *scale* 5 cm. **h** Deformation in microbial mats resulting from the formation of desiccation cracks or from uneven growth; *scale* 1 cm. **i** Undulating dolomitic crusts (marked with *dashed line*). **j** Silicified octracod carapaces in marly dolomite; *scale* 200 μm. **k** Bioclastic-peloidal grainstone in the upper part of an event shell accumulation. Note individual recrystallized shells (convex-up orientation) and abundant ostracod carapaces; *scale* 4 mm. **l** Polished slab of a nodular limestone bed at the transition to the Varnytsya Fm.; *scale* 1 cm. **m** Vertical structure of an event shell accumulation; *scale* 5 mm

1. laminated sediments;
2. deposition in conditions of oxygen depletion (as indicated by abundant organic matter);
3. massive carbonates;
4. dominance of microbialites;
5. marginal or reworked basal deposits;
6. an apparent lack of well-defined sequences or sedimentary subenvironments (Tucker 1978; Valero-Garcés and Aguilar 1992);
7. lack of fauna or restricted, monospecific assemblages, composed predominantly of ostracods and soft-bodied burrowing fauna;
8. lack of evidence of tidal activity in spite of shallow-water environment (Tucker 1978);
9. high lateral variability.

It is difficult to confirm the lacustrine nature of a pre-Devonian basin, given that indicative organisms specifically adapted to such environments had not yet evolved. Coastal lakes and ponds, however, are a ubiquitous (although individually ephemeral) element in the geomorphology of tropical carbonate platforms (e.g., Dix et al. 1999). Strongly depleted $\delta^{13}C_{carb}$ values (up to −10.53 ‰) indicate intensive biological fractionation, which is in agreement with the dominance of stromatolites throughout the formation and the high content of organic matter (especially in the basal part). The environment is envisaged as an enclosed lagoon or coastal lake rather than an open-marine (although extremely epeiric) environment, because the latter would require that both sea-floor anoxia and a benthic microbial carbonate factory developed in the subtidal zone (compare Calner 2005a). Small bodies of water are much more prone to develop restricted conditions and respond to seasonal climatic changes, which are reflected in depositional cyclicity, as observed in the Prygorodok Fm. with respect to redox conditions. An extremely calm environment, which allowed sedimentation from suspension and preservation of bentonite beds, as well as the lack of evidence for tidal or wave activity in spite of the very shallow depth, also support the proposed interpretation.

The Varnytsya Formation

Deposits representing the Varnytsya Fm. were recognized in the Kudryntsi-Castle outcrop. The boundary with the underlying Prygorodok Fm. can be found in the Kudryntsi-Cowpath and Milivtsi–South and North (Fig. 4l) sections as a nodular limestone bed in the lowermost part of the Kudryntsi–Castle section (Figs. 2, 7), marking the beginning of fully developed peritidal deposition. In the most continuous section, Kudryntsi–Castle, 6-m-scale cycles have been recognized and an idealized cycle is presented in Fig. 8. Since the top of the formation is not exposed in the area, the exact thickness of the Varnytsya Fm. could not be determined, but it is at least 24 m.

Subtidal facies

Two different facies have been distinguished in the subtidal deposits of the Varnytsya Fm.: deeper-water, nodular limestones, and shallower-water, stromatoporoid-tabulate coral biostromes. In the lower part of the Varnytsya Fm., biostromes are absent and nodular limestones are depleted in shelly fauna. Faunal diversity increases along with the development of biostromes towards the top of the section.

Nodular limestones (NL in Table 3) are characterized by dark, hard nodules embedded in a lighter, marly matrix. The nodules are formed by bioclastic mudstone to packstone, commonly with peloids (Fig. 7c). They form continuous layers in the lower part of each bed and become disrupted towards the top (Fig. 7b), where they are penetrated by burrows lined with bioclasts, which are commonly selectively dolomitized.

The shallow subtidal facies is represented by stromatoporoid-tabulate biostromes and bioturbated bioclastic limestones containing abundant brachiopods, ostracods, crinoids, bryozoans, rugose corals, and rare fragments of trilobites (BW and PBGW in Table 3). The thickness of biostromes does not exceed 1.5 m. They intercalate laterally with bioclastic limestone, which exhibits an increasing degree of environmental restriction, reflected by a decreasing diversity of fossils and increase in numbers of beyrichid ostracods (OWP and OM in Table 3; Fig. 9k–m). Bryozoans and tabulate corals are fragmented, indicating

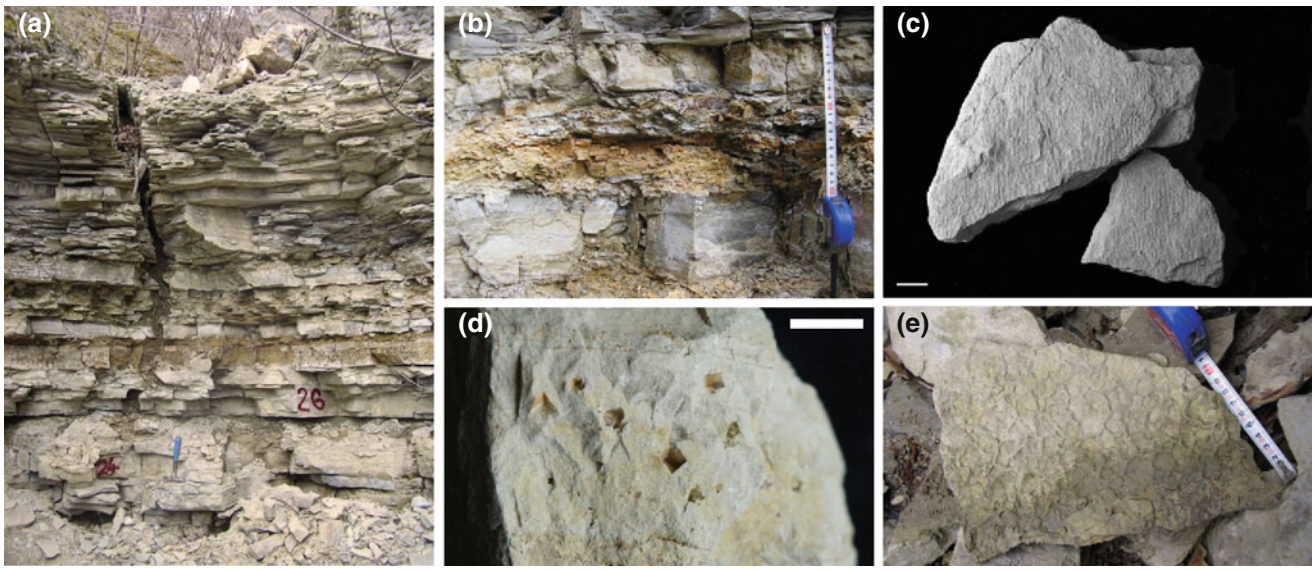

Fig. 5 The Milivtsi—South section. **a** The decimeter-scale bedded marly dolomicrite forming the bulk of the Prygorodok Fm; *hammer* for scale. **b** Orange-colored metabentonite bed; *measuring tape* shows 20 cm. **c** Wrinkle structures on a bedding plane within marly dolomicrite. **d** Angular pores occurring in one horizon within marly dolomite, interpreted here as halite casts; *scale* 1 cm; **e** dense crinkled structures resembling mud cracks, abundant on bedding planes within the upper part of the Prygorodok Fm.; measuring tape shows 10 cm

shoreward or off-biostrome transport. The transition to the intertidal facies (see below) is associated with peloidal-bioclastic wackestone-grainstone (PBWG in Table 3; Fig. 7d), which is interpreted as lagoonal sediment formed in conditions of increasing salinity and restricted circulation, but under wave action. The boundary with the overlying laminites is often developed as an erosional surface in partially lithified mud, covered with a flat-pebble conglomerate (LBFR in Table 3; Fig. 7g).

Intertidal facies

The intertidal facies is represented by stromatolitic dolomite and limestone (DSB in Table 3; Fig. 9b) and ostracod mudstone (OM in Table 3; Fig. 9k). Almost no trapping of detrital sediment was observed in the laminites. This indicates very high rates of accumulation of autochthonous carbonate. The presence of desiccation cracks and flat-pebble conglomerates (LBFR in Table 3; Fig. 7g) indicates that the sediment was subjected to periodic subaerial exposure, and that lithification within the microbial mat was rapid. The intertidal deposits are barren, except for rare eurypterids and ostracods (Fig. 9k).

Supratidal facies

The boundary between intertidal and supratidal deposits is gradual and placed within the laminite facies. The following features distinguish the supratidal facies: (1) internal breccia composed of angular intraclasts embedded in orange, clayey matrix (SBB in Table 3; Fig. 7e, h); this breccia is interpreted as resulting from sediment fracturing during evaporite growth and collapse following its dissolution; (2) abundant mudcracks; and (3) horizons of cavities filled with an easily disintegrating argillaceous, porous marl. These horizons are usually conformable with bedding, but locally affect several adjacent beds. The porosity seems to result from dissolution of evaporite minerals.

Additionally, two horizons exhibit a sequence indicative of regolith formation. The sequence starts with 1–2 cm of dark brown mudstone (Fig. 7f), capped with a thin, creamy claystone crust with iron oxide spotting, devoid of carbonate. Up to 10-cm-long coalified stems, tentatively identified as *Primochara calvata* T. Ishchenko, 1975, are preserved in these beds, which are otherwise devoid of macroscopic fossils.

The $\delta^{13}C_{carb}$ values in the Varnytsya Fm. have been measured only in nodular limestones and were all negative (ranging from −0.33 to −3.20 ‰).

The Zavalya section

The Zavalya section consists of two outcrops located at a distance of ca. 600 m apart on the same valley slope. The

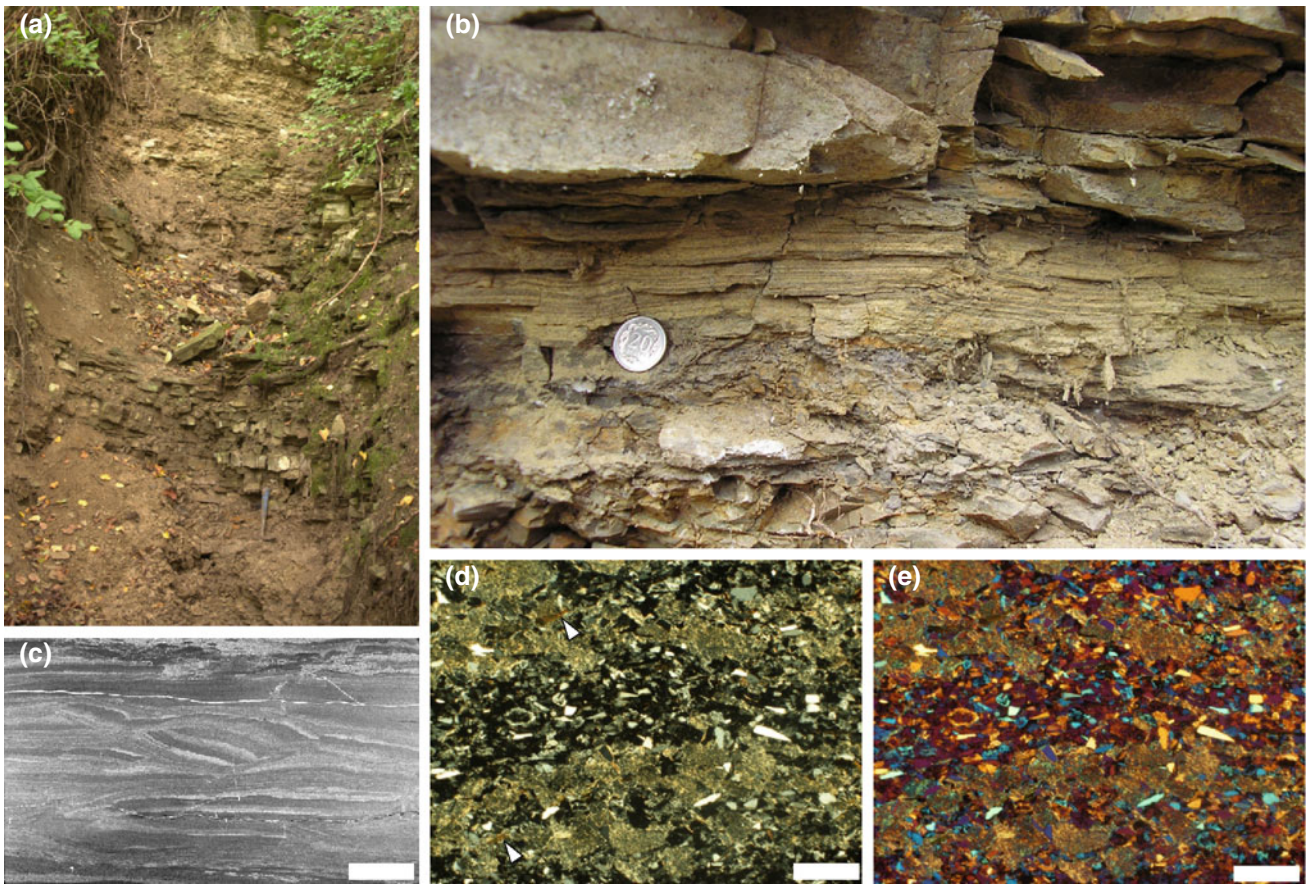

Fig. 6 The Prygorodok Fm. in the Kudryntsi—Cowpath section. **a** General view of one of the adjacent ravines which form the exposure, *hammer* for scale. **b** Laminated volcanogenic bed, *coin* diameter 18 mm. **c** Cross bedding in laminated dolomicrite, indicating current action; *scale* 5 mm. **d** Microfacies of the laminated volcanogenic sediment: quartz layers contain angular, moderately sorted grains belonging to the very fine sand fraction, together with biotite flakes (*arrows*) aligned parallel to bedding; plane polarized light, *scale* 500 μm. **e** As in **d**, with gypsum plate inserted

basal part of the Zavalya 2 section (Figs. 2, 3) is developed as massive bioclastic-lithoclastic grainstone (BLG in Table 3; Fig. 10b–d). The grain-supported fabric is formed by fragmented and slightly abraded shells, some intensively bored (Fig. 10c). Sorting changes gradually within a given bed, from very well sorted and aligned shell fragments to a moderately sorted mixture of shells and rounded mudstone and peloidal grainstone extraclasts. There are also rare tangential and slightly eccentric ooids with sparry or micritized cortices (Fig. 10b). In view of the small size of the outcrop, it was not possible to observe macroscopic sedimentary structures, such as cross-bedding. These facies would be readily interpreted as shoal or levee deposits, if not for horizons of very high secondary porosity due to dissolution vugs, which expand primary pores and also affect bioclasts (Fig. 10d). At least two generations of blocky calcite cement are present. The first generation of cement, which surrounded original shells, preserves the empty voids left after their dissolution. The second generation fills these empty voids, and is gravitational, indicating a vadose diagenetic environment. The rocks were therefore deposited either as bioclastic shoals which became emergent, or were originally formed as beachrocks.

The grainstone is overlain by several low-relief stromatoporoid-tabulate biostromes (STP in Table 3; Fig. 10e). The interval directly above the biostromes is not exposed (Fig. 2, 3). The upper part of the outcrop begins with bioturbated bioclastic wackestone to packstone (BW in Table 3) with a diverse fully marine fauna, including bryozoans, nautiloids, brachiopods, gastropods, calcareous algae (Fig. 9h–j), crinoids, and ostracods (Fig. 9e). This facies represents the subtidal zone and is succeeded by thick beds of dolomitic laminites of the intertidal zone, with dissolution breccia of the same type as described

Table 3 Microfacies of the Ludfordian deposits in the Zbruch River Valley

Microfacies	Texture	Grains	Matrix	Diagenetic features
RD Replacement dolosparite Fig. 4c	Dolosparite non-mimically replacing originally bioclastic limestone (Fig. 4c)	Ghosts of skeletal grains preserved as dark and finely crystalline areas. Recrystallized ostracod shells form cap-in-cap structures and concentrated in layers	Planar, subhedral to euhedral inequigranular, tightly packed dolosparite	Two main classes of crystal sizes: 50–200 μm in the replaced matrix and shells, and 500–1000 μm in voids filled with cement. Rare, bedding-parallel, anastomosing, sutured clay seams
IWR Intraclast wackestone-rudstone Fig. 4e	The texture varies from wackestone to rudstone depending on the degree of brecciation, which ranges from lithoclasts remaining almost in situ with slight fractures to heavily crushed and overturned gravel, giving them seismite-like appearance	Sharp-edged, angular clasts of marl and siltstone, millimeter- to centimeter-sized, often laminated. Clast positions suggest slumping and sliding with respect to each other. Rare dolomite rhombohedra and mica flakes are scattered in the matrix and concentrated in layers	Brown argillaceous micrite with flakes of organic matter, dense mesh of internal fractures. Intercalations of pure marlstone with high porosity	Brecciation in this microfacies seems synsedimentary, and is therefore not considered a diagenetic feature
LMQ Laminated mudstone with quartz Figs. 4h, 6c	Mudstone with an admixture of silt-sized quartz. Microbial mat growth indicated by preservation of load casts and uneven growth; also mechanical lamination indicated by cross-bedding	Quartz grains in the matrix and concentrated in laminae, where they are larger (20-30 μm) and their sorting is poor. Admixture of biotite flakes and flocks of amorphous organic matter	Laminated, argillaceous microcrystalline dolomite	
BRG Bioclastic rudstone to lithoclastic-peloidal-bioclastic grainstone Fig. 4k, m	Characteristic vertical structure: the bottom boundary is an erosional surface penetrated by cracks infilled with overlying sediment (Fig. 4m). Above, grains show normal grading: bioclastic rudstone at the bottom, grading upwards into grainstone and finally packstone. The thickness of the entire sequence does not exceed 10 cm	Bimodal sorting: the larger fraction composed of gastropod and bivalve shells, disarticulated but not crushed, and fragments of bryozoans. Bivalve shells are arranged predominantly convex-up (Fig. 4m). The finer fraction consists of ostracod carapaces, peloids, well-rounded lithoclasts and small gastropods. Some shell cavities are filled with micrite or peloidal grainstone, others show geopetal structures. Some shells shelter fragments of mudstone in different orientations, showing that they were derived from at least partly lithified sediment	In the bottom part, the matrix is inequigranular xenotopic to hypidiotopic calcite spar	Gastropod and bivalve shells are completely recrystallized with blocky xenotopic calcite spar filling the voids outlined by finely crystalline cement or micritic rims formed due to microboring. Most grains cemented by inequigranular to blocky hypidiotopic calcite spar. Others have constructive micritic envelopes. Some bioclasts silicified
BLG Bioclastic-lithoclastic grainstone Fig. 10b	Grainstone	Very poorly sorted mixture of rounded extraclasts, representing mudstone and peloidal grainstone, and of fragmented and slightly abraded shells. As shell cavities shelter micrite accretions, they are likely derived from at least partly lithified sediment	Inequigranular hypidiotopic calcite spar	Most shells are recrystallized, but many have preserved micritic rims. Grains are surrounded by circumgranular isopachous bladed cement layer

Table 3 continued

Microfacies	Texture	Grains	Matrix	Diagenetic features
OM Ostracod mudstone Fig. 9k	Mudstone. Brownish streaks in the matrix and arrangement of bioclasts underline planar, wavy sedimentary bedding. Horizontal, centimeter-sized bioturbations marked by clay seams and filled with peloids and more abundant shell debris	Poorly sorted ostracod carapaces, articulated and fragmented, peloids, and sparse fragments of tabulate corals and brachiopod shells. Coalified fossils visible in cross-cuts	Microspar, locally with fenestral or clotted fabric, which might be of thrombolytic origin	Bioturbation is selectively affected by dolomitization and rich in dissolution vugs rimmed by microcrystalline and blocky cement. Barren areas contain pseudomorphs, the shape and twinning of which indicate sulphate minerals, i.e., gypsum or celestite
OWP Ostracod wackestone-packstone with bioturbation Fig. 4f, j, 9l, m	Bioturbated wackestone-packstone, clotted	Ostracods, locally forming cap-in-cap structures, peloids and lithoclasts, very poorly sorted, predominantly fragmented. Lithoclasts are well rounded and represent unfossiliferous mudstone	Micritic, patches of microspar	Rare gastropod shells are completely recrystallized to blocky calcite spar. Bioturbation is underlined by areas selectively affected by dolomitization, less fossiliferous and with boundaries marked in places by clay seams
DSB Dolomitized stromatolitic boundstone Fig. 9b	Millimeter-sized laminae parallel to bedding or disrupted and imbricated by current or forming gas-escape structures. Lighter laminae have spotted or polymodal planar-euhedral fabrics with empty pores between crystals. Darker laminae very fine-grained, equigranular and sutured	No grains	Fine- to medium crystalline hypidiotopic dolosparite	
LBFR Lithoclastic-bioclastic floatstone-rudstone with peloids Fig. 7g	Imbricated flat-pebble conglomerate, upwards grades into mudstone. Typically deposited over an erosive surface	Angular, flat fragments derived from algal mats and fragments of shells, echinoderms and tabulate corals. In some sections also peloids. Grains form tightly packed aggregates and exhibit on their contacts traces of dissolution due to compaction	Micrite or microspar	
PBWG Peloidal-bioclastic wackestone-grainstone Fig. 7d	Peloidal-bioclastic wackestone-grainstone	Small ostracods, echinoderm fragments, and putative foraminifers	Grades from fine microspar to inequigranular hypidiotopic calcite spar	Highly porous rock—pores are likely leached bioclasts. Clay seams
BUM Bioturbated unfossiliferous mudstone	Mudstone with bioturbations visible as patches of darker, porphyrotopic fabrics with very finely crystalline to microcrystalline dolomicrite scattered with sub-millimeter-sized crystals	Sparse quartz grains scattered in the matrix and concentrated in clay seams	Dolomicrite grading to equigranular dolosparite	Clay seams and fenestral vugs concentrated in areas rich in silt, suggesting that they were formed by mechanical or chemical removal of clay. This microfacies occurs also as internal breccia composed of angular and subangular intraclasts with many voids and fractures filled with insoluble residue and with blocky cement

Table 3 continued

Microfacies	Texture	Grains	Matrix	Diagenetic features
BW Bioclastic wackestone Fig. 9e–i	Wackestone with bioturbation	Poorly sorted bioclasts, with a small proportion of large, articulated ostracods and brachiopods and numerous small and fragmented ostracods, tabulate corals, bryozoans and calcifying algae, incl. *Tuxekanella simplex* and *Hedstroemia*. Many grains have cyanobacterial coatings. Single conodonts were also found in a thin section	Micrite, little microspar	
NL Nodular limestone Fig. 4l,7b, c, 9d	Bedding-parallel intercalations of marl and micritic limestone layers, either completely unfossiliferous, or developed as bioclastic-peloidal mudstone-wackestone. (Crypto)bioturbation underlined by bioclasts and peloids, either restricted to non-clayey layers or extend from clayey layers downwards as digitations. Contacts between the two types of layers range from very gradual to sharp boundaries with fractures infilled with sparry cement or geopetally with clay residue. In the latter case, bioclasts do not cross the boundary and are truncated by dissolution (Fig. 7c)	In mudstone-wackestones the bioclasts include predominantly ostracods, poorly sorted and preserved as articulated or disarticulated, but not fragmented shells. In some cases, marly layers contain the same fauna, showing no signs of compaction	In limestone layers the matrix is micrite to microspar	Shells are replaced with micrite or blocky spar. Burrows are often selectively dolomitized. The rock is cut by numerous fractures filled with cements, some fractures grade into clay seams. The general direction of fracturing is vertical and sub-vertical. Some fractures are also truncated at the boundaries with clayey layers
STP Stromatoporoid-tabulate packstone Fig. 10e	Packstone with stromatoporoids and tabulate fragments, both in situ and reworked	Poorly sorted, chaotically arranged: articulated and fragmented ostracods and brachiopods, crinoid ossicles, echinoderm spines and trilobite carapaces. Common encrustation by *Girvanella*	Argillaceous micrite	Many bioclasts have micritized rims. Clay seams and tangential contacts between grains indicate some degree of compaction
SBB Stromatolitic boundstone breccia Fig. 7h	Microbially laminated with deep (>10 cm) cracks penetrating the rock, forming irregular polygons, filled with ostracod wackestone. The sediment is crossed by laminae, which converge with the increasing degree of dissolution, forming clay seams, “horsetail” structures and swarms	Microbial laminae are generally devoid of fossils, but some contain concentrations of small, well-sorted ostracod carapaces and peloids. The cracks are filled with large ostracods and peloids	Partly dolomitic micrite	Crack edges are marked by clay seams, but not by cements, suggesting that they were filled with penecontemporaneous sediment and have likely undergone subsequent dissolution. The rock is porous due to dissolution vugs filled completely or geopetally with microcrystalline or blocky cement. Many vugs are developed from fissures enhanced by dissolution, characterized by predominantly vertical direction

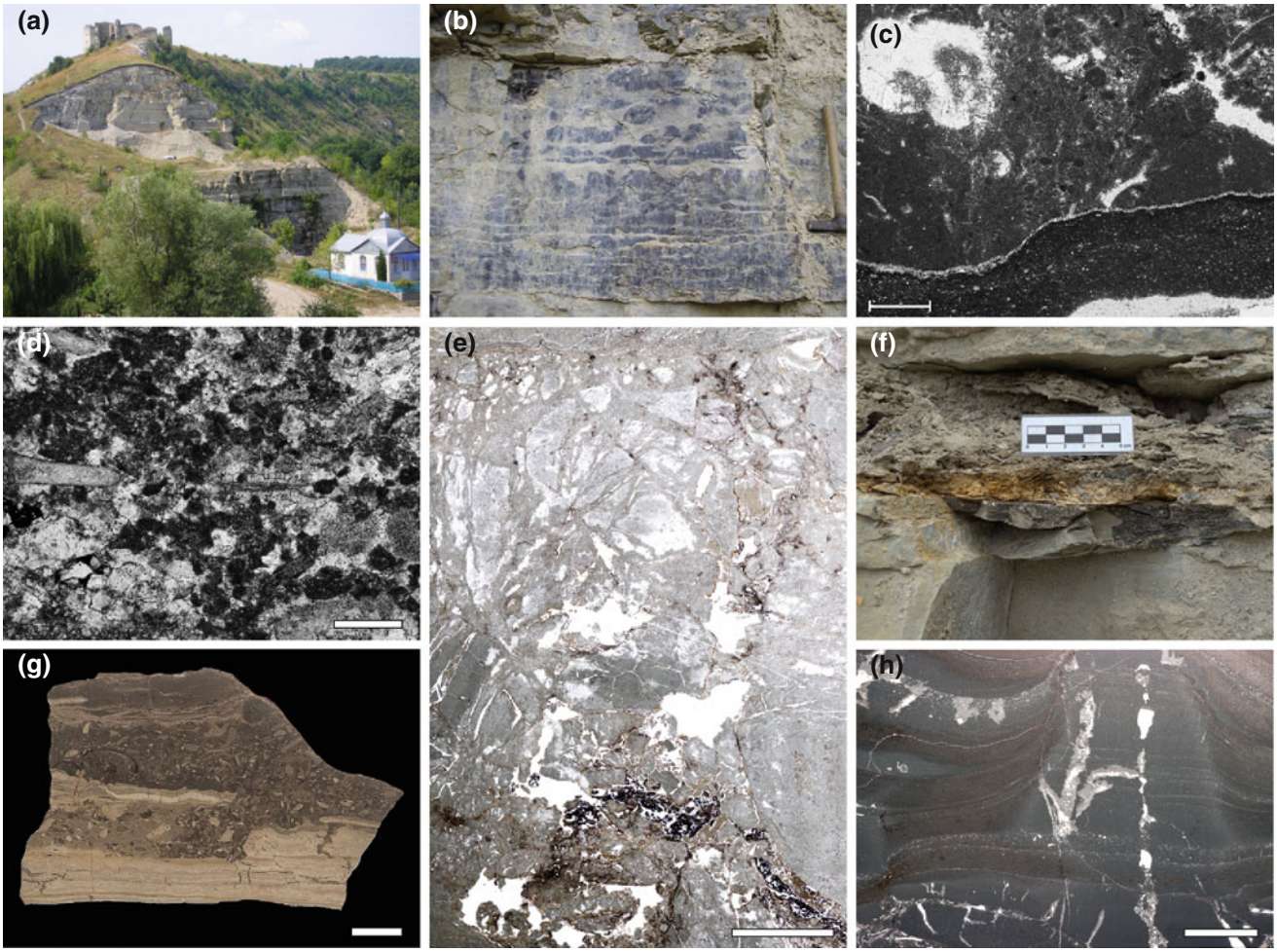

Fig. 7 The Kudryntsi–Castle section. **a** View of the quarry, total height is approx. 24 m. **b** Nodular limestone bed, *hammer* for scale. **c** Nodular limestone—cemented contact between a nodule (*top*) and marly matrix (*bottom*), *scale* 500 μm. **d** Peloidal-bioclastic grainstone (PBWG in Table 3) with two types of calcareous microproblematica: one funnel-shaped and one ostracod-like (compare Fig. 9f), *scale* 200 μm. Supratidal zone. **e** Collapse breccia resulting from dissolution of evaporites, *scale* 5 mm. **f** Organic-rich mudstone with reworked clasts of underlying rock and coalified stems of *Primochara calvata(?)*, overlain by claystone; *scale* 5 cm. **g** Lithoclastic-bioclastic floatstone-rudstone with peloids (LBF in Table 3); *scale* 1 cm. **h** Stromatolitic boundstone breccia (SBB in Table 3), *scale* 5 mm

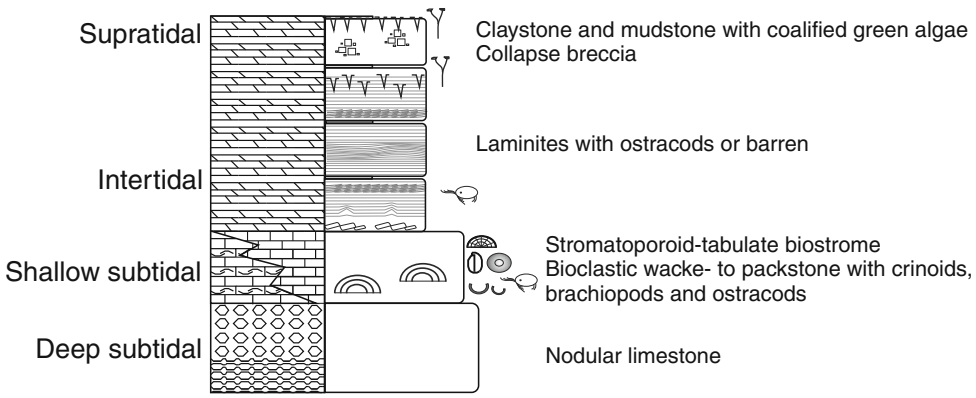

Fig. 8 Idealized peritidal cycle of the Varnytsya Fm

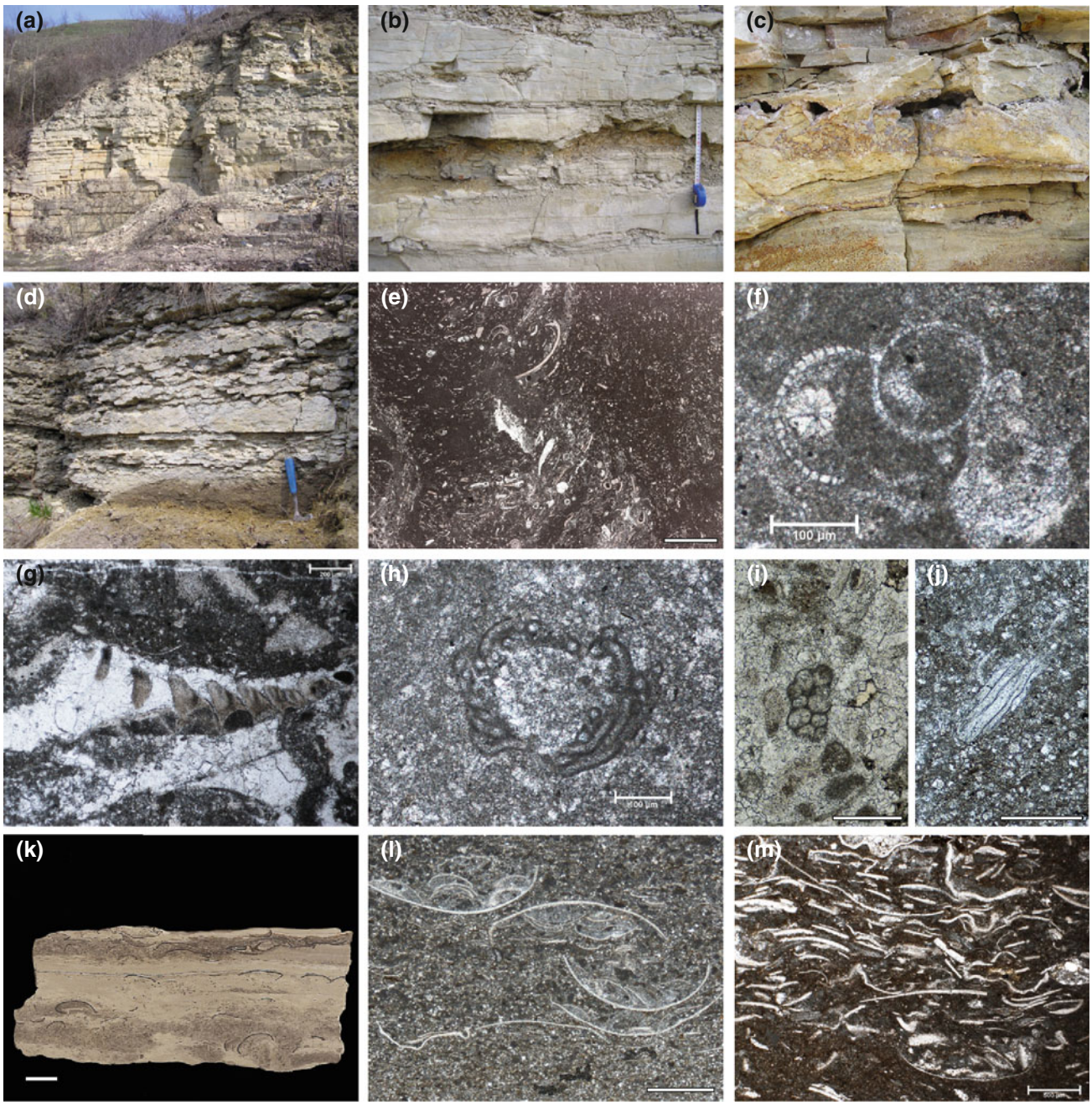

Fig. 9 The Zavalya 1 section. **a** Overview of the outcrop. The height is ca. 21 m. **b** Horizons of cavities filled with clayey residue rich in iron oxide formed in dolomitic laminites; tape shows 20 cm. **c** Collapse breccia composed of angular clasts of the surrounding dolomite, cemented by sparry calcite and red clay. **d** Nodular limestone bed; *hammer* for scale. **e**–**h** Bioclastic wackestone (microfacies BW in Table 3). **e** Bioturbation indicated by the arrangement of bioclasts. **f** Microproblematicum resembling an unusual ostracod shell associated with *Microcodium*; *scale* 100 µm. **g** Cross section through a conodont element, *scale* 200 µm. **h** Calcified cyanobacterial tubes resembling *Girvanella*; *scale* 100 µm. **i** Cross section through a bundle of calcified tubes of *Tuxekanella simplex* Riding and Soja (1993), *scale* 100 µm. **j** Longitudinal section through a bundle of *T. simplex*; *scale* 100 µm. **k** Polished slab of an ostracod mudstone (OM in Table 3) from the intertidal zone; *scale* 1 cm. **l**, **m** Ostracod wackestone-packstone (OWP in Table 3). **l** Cap-in-cap structures formed by ostracods; *scale* 200 µm. **m** Accumulation of leperditicopid and beyrichid ostracods; *scale* 500 µm

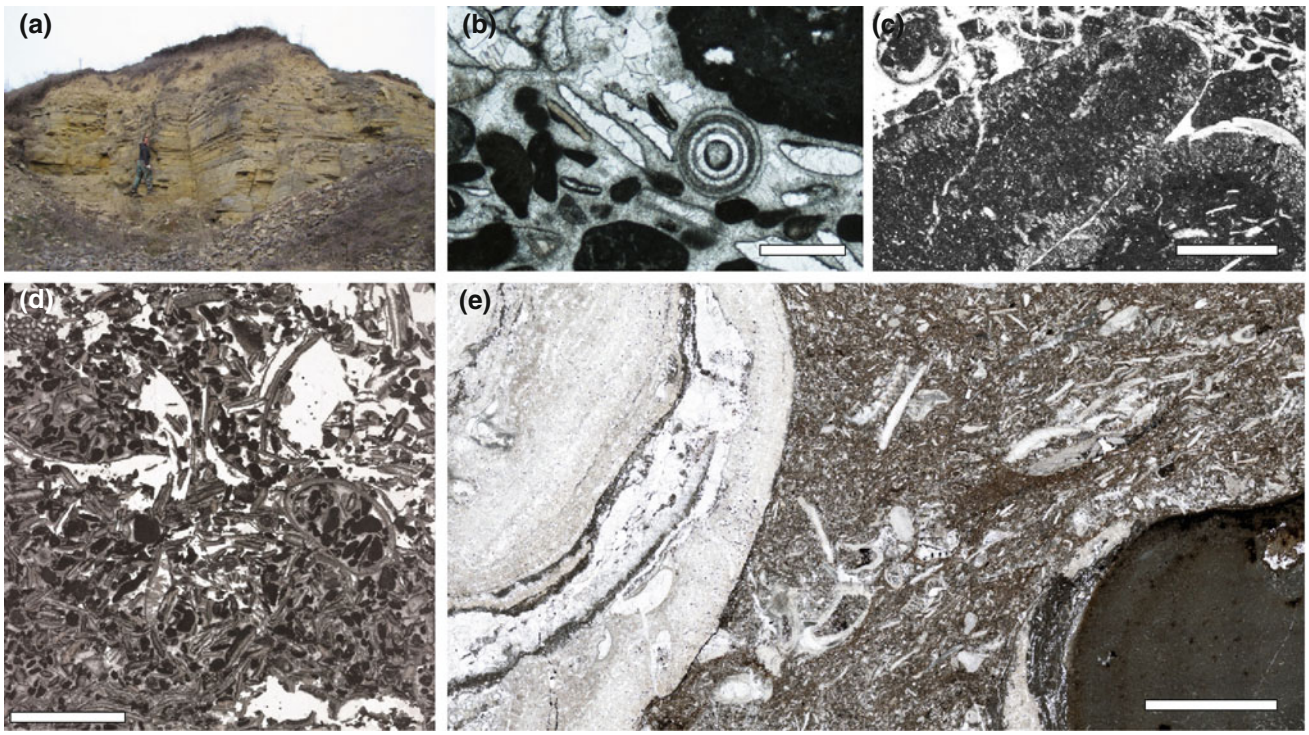

Fig. 10 The Zavalya 2 section. **a** Outcrop view; the height is approx. 8 m. **b–d** Bioclastic-lithoclastic grainstone (BLG in Table 3). **b** A tangential and slightly eccentric ooid; *scale* 500 μm. **c** *Scale* 200 μm. **d** *Scale* 5 mm. **e** Stromatoporoid-tabulate packstone (STP in Table 3). The stromatoporoid is encrusted and penetrated by *Girvanella* tubes; *scale* 5 mm

above from the Varnytsya Fm. (Fig. 9b, c). In the upper part of the section, the fauna of the subtidal zone is reduced almost exclusively to beyrichid ostracods, commonly forming dense shell beds (Fig. 9k–m).

In the lower part (Zavalya 2), $\delta^{13}C$ values are close to 0 (−0.64 and −0.84 ‰). In the upper part of the section (Zavalya 1), $\delta^{13}C$ values reach +2.77 ‰ in the nodular limestone bed (Fig. 9d), and drop back to low negative (−1.03 ‰) in the marls above.

Discussion

Depositional environment of the Prygorodok Formation

The thickness of the deposits belonging to the Prygorodok Fm. in the studied area reaches 16 m. Low-energy sedimentation and the lack of a proper benthic carbonate factory of Paleozoic-type raise questions about the main sediment source. As no facies models for Silurian carbonate lakes exist, this environment will be discussed here in more detail.

Typically, for carbonate coastal lakes, the following mechanisms of sediment accumulation are considered (Gierlowski-Kordesch 2010):

1. fluvial input and surface runoff;
2. aeolian input;
3. material transported shoreward from the sea by hurricanes and tsunamis;
4. carbonate precipitation through biogenic mediation;
5. evaporation.

Tempestites occur in the Prygorodok Fm. as a subordinate component, and the evidence for evaporite growth is limited to cubic voids, interpreted as pseudomorphs left after halite dissolution (Fig. 5d). The presence of evaporites and lack of sedimentary structures characteristic of fluvial facies also makes the fluvial input less likely.

The bulk of the Prygorodok Fm. is dolomicrite. Dolomite precipitation from sea water through the activity of microorganisms is a likely mechanism. Their role in precipitation of dolomite has been attributed to the removal of sulphate by sulphate-reducing bacteria (Vasconcelos and McKenzie 1997; Van Lith et al. 2003; Sanz-Montero et al. 2008), but recent studies point to the organic matrix provided by microbial mats as the crucial factor. The site where microbial dolomite precipitation was originally observed (Lagoa Vermelha, Brazil) closely resembles the environmental model proposed here for the deposition of the Prygorodok Fm. in terms of climatic setting and hydrologic conditions. The site is an isolated lagoon with salinity that fluctuates with the evaporation/precipitation

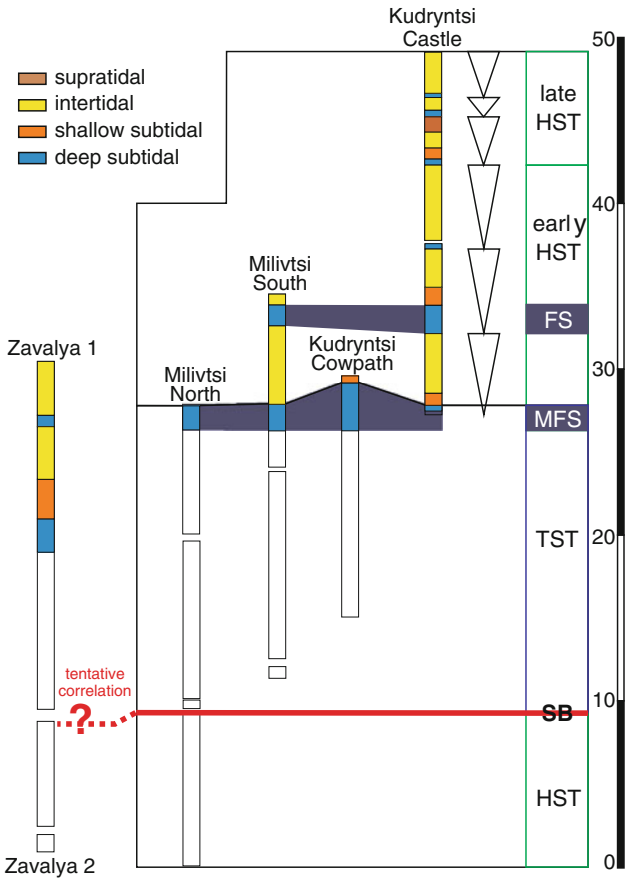

Fig. 11 Summary of sections with sequence-stratigraphical interpretation for the Kudryntsi–Castle section. *HST* highstand systems tract, *TST* transgressive systems tract, *SB* sequence boundary, *MFS* maximum flooding surface, *FS* flooding surface

ratio in the wet and dry season, and depends also on the proportions of meteoric and marine waters in the groundwater supply (Vasconcelos and McKenzie 1997). In view of the relative novelty of modern analogue, few fossil examples of such a lacustrine-lagoonal environment have been recognized. Many ancient dolomite occurrences exhibit features associated with syndepositional or early diagenetic formation of dolomite under anoxic conditions and with a distinct cyclic microfacies pattern, which may correspond to the development and demise of microbial communities or seasonal climate rhythms (Vasconcelos and McKenzie 1997). Therefore, it seems likely that more fossil analogues may be identified in the future.

Laminae of organic matter enriched in silt- and fine sand-sized quartz grains in the lower part of the unit indicate that in the early stages of deposition the basin underwent stratification with respect to redox conditions, with repeated episodes of sediment oxidation associated with the influx of silt-sized fluvial or aeolian clastic material. This stratification regime was probably not maintained during deposition of the massive, argillaceous dolomite with bioturbation.

In the mid- to upper part of the Prygorodok Fm., leperditicopid ostracods in the massive dolomite facies, together with bioturbation, indicate that the factor(s) which limited the development of a more diverse fauna were not dysoxia. Salinity is another likely restrictive factor. Ephemeral coastal lakes are typically unstable environments subject to drastic hydrological fluctuations. The cubic casts found in the Milivtsi–South section (Fig. 5d) are the only sedimentary evidence for elevated salinity. Westwards across the strike, Tsegelnyuk et al. (1983, p. 68) reported the occurrence of translucent gypsum and anhydrite in boreholes corresponding to the Prygorodok Fm. In younger deposits, the nature of the biota is often a useful reflection of the salinity regime, but no proper freshwater ecosystems existed in the Silurian. The association of ostracods and microbialites in the absence of other organisms may indicate elevated or reduced salinity. Monospecific leperditicopid ostracod assemblages are typical indicators of restricted settings, such as confined lagoons and environments affected by periodic subaerial exposure (Vannier et al. 2001). It is not possible at this point to confirm the salinity regime of the basin during deposition of the Prygorodok Fm. Lack of fauna or low-diversity assemblages could be explained by any one of three factors: unfavorable redox conditions, a yet to be filled Silurian ecospace, or finally, nutrient deficiency. The latter has been evoked as a possible explanation for the barren character of Paleozoic lake environments (Park and Gierlowski-Kordesch 2007).

In addition to biologically mediated dolomite precipitation, a subordinate aeolian admixture is represented by the bentonite beds and by the laminated fine-grained sandstones-claystones of volcanic origin (Fig. 6d, e). Silt-sized quartz admixture visible in the laminated mudstone, which locally forms sheet-like beds several centimeters thick, cemented with carbonate and stabilized by undulating dolomitic microbial crusts, is also a possible candidate for an aeolian origin. Over-representation of wind-derived sediment may reflect increased dustiness coincident with the Ludfordian CIE, as proposed by Kozłowski and Sobień (2012, see discussion therein).

The record of sea-level changes

Studied sections are presented in Fig. 2 along with a correlation based on topographic position, lithology and stable carbon isotope trends (Fig. 11). In spite of the facies model of Einasto et al. (1986), where the Silurian carbonate platform of Podolia is treated as rimmed, it is assumed here that a carbonate ramp is a more appropriate model due to the very low-relief and spatial discontinuity of the biostromes and reef mounds and the epeiric character of the Podolian part of the basin (compare Eriksson and Calner 2008; Skompski et al. 2008).

The first recognizable element of stratal architecture is the sequence boundary (SB) marking the top of the Isakivtsy Fm. The second element is the stacking pattern recorded in the peritidal deposits of the Varnytsya Fm. Figure 11 shows changes in cycle thickness, which, it is assumed, reflect the amount of accommodation space available. The first three cycles show an aggradational stacking pattern, which is a characteristic feature for early highstand systems tract (HST). The next three cycles are substantially thinner and exhibit in their upper parts extensive evidence of subaerial exposure, indicating a gradual loss of accommodation, typical of the late HST. The entire cyclic sequence is interpreted as HST, with the first three cycles having been deposited during a sea-level stillstand, and the following three, during a relative sea-level fall.

The Prygorodok Fm. does not record the depositional processes, which took place following the sea-level fall and subaerial exposure of the Isakivtsy Fm. It is likely that the sedimentary gap above the sequence boundary corresponds with deposition of a falling stage systems tract farther down the ramp, followed by a lowstand systems tract. The Prygorodok Fm. deposits would therefore represent the transgressive systems tract (TST), ending in the maximum flooding surface (MFS) clearly distinguishable in all sections as a condensed, fossiliferous nodular limestone bed (Fig. 11). Subsequent to this peritidal facies represent the HST and the transition from the Prygorodok Fm. to the Varnytsya Fm. In the present study, no sedimentological features were found which would point to when the open-marine waters transgressed into the Prygorodok lagoon or lake basin. The upper part of the formation is developed as microbial laminites with numerous traces of exposure, resembling the supratidal zone deposits of the Varnytsya Fm.

The position of the Zavalya section

The dolosparite of the Isakivtsy Fm., exposed north of Milivtsi as a single, nearly continuous outcrop over a distance of 1.3 km, does not outcrop elsewhere in the studied area. Geometrically, the Zavalya 1 section corresponds to the topographic level at which the Isakivtsy dolomite is found, however, the facies in the Zavalya 1 section are entirely different. They represent peritidal deposits resembling the Varnytsya Fm. described above, with the topmost part dominated by marly, stromatolitic dolomite with a monospecific ostracod fauna. The combined Zavalya 1 and 2 sections and the Isakivtsy-Prygorodok transition show opposite sea-level trends: the Zavalya section starts with the facies deposited in a shallow, but marine environment with fully developed biostromes (Fig. 10), and grades into marginal-marine deposits with evidence of exposure and evaporite formation (Fig. 9b, c), and can be therefore summarized as regressive, whereas the Prygorodok-Varnytsya transition represents late transgressive to highstand conditions. Moreover, $\delta^{13}C$ values in the Varnytsya deposits, both in this study (Fig. 2) and reported from neighboring sections (Kaljo et al. 2007, 2012), are close to 0 or slightly negative, whereas the data here record a positive peak (+2.77 ‰, value from brachiopod shell) in the upper part of the section, supporting its position at the level of the CIE at the Isakitvtsy-Prygorodok boundary.

As the Isakivtsy Fm. is clearly defined based on diagenetic features, it cannot be ruled out that the deposits in Zavalya represent the same original facies that have not undergone dolomitization. The lateral distance between the two sections is ca. 6.5 km (approximately along the strike). A possible reason for patchy spatial distribution of dolomitization might be a reflection of lateral variability of the overlying Prygorodok Fm., supporting the presented environmental interpretation.

Relationships with the global facies record and eustatic trends

The sequence boundary present at the Isakivtsy-Prygorodok transition, recording prolonged exposure of the carbonate platform, may be correlated with the widely observed sea-level fall coincident with the base of the mid-Ludfordian CIE (see review in Loydell and Frýda 2011). In the carbonate succession of Gotland this event is recorded as an erosion surface at the Hemse/Eke boundary (Jeppsson et al. 2007) and the occurrence of grainstone and stromatolites, and dissolution pipes, indicating karstification in the overlying Lower Eke Fm. (Cherns 1982; Eriksson and Calner 2008). In the clastic carbonate succession of the Rzepin section in the Holy Cross Mountains (Kozłowski and Munnecke 2010) the SB interval is developed as the sandy-oolitic Jadowniki Member, which contains numerous erosive surfaces and signs of subaerial exposure in the top of the oolite-bearing unit (e.g., keystone vugs, Kozłowski 2003; Kozłowski and Munnecke 2010). In the Shropshire area (UK), the pronounced positive excursion in organic carbon isotopes occurs near the Ludlow Bone Bed and is followed by progradation of the Downtonian facies (Loydell and Frýda 2011).

In the case of more distal depositional settings, common shallowing-upward facies trends are observed near the base of the CIE (Scania—Wigforss-Lange 1999; Australia—Jeppsson et al. 2007); however, the shallowing trends in these cases continues also above the onset of the CIE (Martma et al. 2005; Kozłowski and Sobień 2012), indicating prolonged progradation during the sea-level lowstand (Kozłowski and Munnecke 2010).

It is important to note that the sections mentioned above represent foreland basin settings with both high

rates of subsidence and sedimentation; hence the sedimentary record includes the sequence boundary and early transgressive deposits. In other cases the gap is more extensive, often encompassing the lower part or the entire CIE interval. In the case of the Prague basin, the shallower facies belt is characterized by erosive-paleokarst surfaces, until the decline of the CIE in the Mušlovka Quarry and probably after the CIE decline in the case of the Požáry Quarry (Lehnert et al. 2007). Similar situations are observed in the proximal shelf of Baltica (Ohesaare drillcore—Kaljo et al. 1997) and Laurentia (Barrick et al. 2010).

In the case of Podolia, regarding the stable carbon isotope stratigraphic data of Kaljo et al. (2007, 2012), the SB is diachronous with respect to the main positive shift of the CIE. It is suggested here that this delay in the placement of the SB results from a deeper-water setting inherited after the flooding interval preceding the regression associated with the Lau excursion and represented by the Grinchuk Fm. deposited in an open-shelf environment. Hence, the regression resulted from both a sea-level fall and filling up of the accommodation space by Isakivtsy sediments.

Sedimentation seems to have been re-established relatively early given the proximal position of studied sections with respect to the Baltica shore, resulting in a more complete record. The stable carbon isotope stratigraphic data of Kaljo et al. (2007, 2012) indicate that the first flooding surface after regression, recorded as the Isakivtsy/Prygorodok boundary is diachronous. The base of the Prygorodok Fm. in the western part of the Dniester valley outcrop area (Isakivtsy-45 of Kaljo et al. 2012) corresponds to the end of the rising limb of the CIE, whereas in the eastern part (5 km to the east, in Braga) the Prygorodok base records CIE decline (Kaljo et al. 2007). Regarding these data and the facies development of the formation in this study, with a slow deepening-upward trend and exposure levels within the succession, the sea-level rise may be interpreted as relatively slow with successive internal flooding surfaces and filling events. This interpretation agrees with the record of the CIE maximum interval in the Holy Cross Mountains, where it is represented by lagoonal sediments of the Bełcz Member and interpreted as early transgressive deposits (Kozłowski and Munnecke 2010). In the case of Gotland, the beginning of the transgression seems to be more prominent (middle and upper Eke Formation, Eriksson and Calner 2008), but it is followed by progradation of the Burgsvik sandstone, which causes the loss of accommodation. In the more distal setting represented by the sediments in the Vidukle drillcore in Lithuania (Martma et al. 2005) biofacies data also suggest the predominance of a progradational-regressive trend, probably accompanied by slowly rising sea level. Spectral gamma ray logs from the open-shelf Mielnik IG-1 core (Kozłowski and Sobień 2012) also indicate the domination of progradational conditions during the entire CIE maximum interval, with terrigenous influx towards the end, consistent with the record from Gotland, Holy Cross Mountains, and the Vidukle core.

The next stage of sedimentation, associated with the end of the CIE decline, which relates to the upper part of the Prygorodok Fm., records in all discussed sections a predominance of transgressive conditions. The facies record in this study area preserves the maximum flooding interval of this transgression in the lowermost part of the Varnytsya Fm., marked by an up to 3-m-thick dark nodular limestones with a more open-marine fauna.

At this level Kaljo et al. (2012) noted minimal $\delta^{13}C$ values, referenced as the "post-Prygorodok isotope low". A similar low in the C-isotope record is observed in the Mielnik IG-1 section (Kozłowski and Sobień 2012) and corresponds with the most pronounced MFSs with condensations of the *Monograptus balticus–Pseudomonoclimacis latilobus* fauna in the offshore setting. Above this level, geophysical and facies data in the Mielnik IG1 section reflect a longer highstand interval. A similar sequence development above the CIE is recognized in Gotland (see Eriksson and Calner 2008, Fig. 10e and related text); therefore the peritidal Varnytsya Fm. may be correlated with the Hamra-Sundre highstand interval.

Conclusions

1. The record of the Ludfordian positive CIE known as the Lau excursion in the Isakivtsy-Prygorodok deposits in the Zbruch River Valley is highly influenced by biogenic carbonate precipitation; the $\delta^{13}C_{carb}$ values in this interval shift strongly towards the negative and constitute an example of facies overprint on the carbon isotope record of sea-water composition.
2. The Prygorodok Fm. is represented by laminated dolomicrite with bentonite and siltstone intercalations, deposited in enclosed lagoons or coastal lakes dominated by microbial mats, which were the main sediment producers, as indicated by $\delta^{13}C_{carb}$ values as low as −10.53 ‰.
3. The Prygorodok Fm. represents TST deposits following a sequence boundary, which resulted from a very rapid regressive event recorded in the Ludfordian of Baltica and other paleocontinents.
4. The Varnytsya Fm. is represented by peritidal facies, encompassing deeper subtidal nodular limestones, shallow subtidal stromatoporoid-tabulate biostromes and bioclastic limestones, intertidal stromatolitic laminites and supratidal regoliths. The $\delta^{13}C_{carb}$ values remain close to 0 ‰ or slightly negative.

5. The sequence boundary in Podolia, which can be correlated across the entire basin (e.g., with Gotland, Holy Cross Mountains), is diachronous with respect to maximum positive $\delta^{13}C_{carb}$ values in the area, reflecting inherited bottom morphology and proximity to the shoreline.
6. The MFS marking the onset of peritidal deposition of the Varnytsya Fm. corresponds to the "post-Prygorodok isotope low" of Kaljo et al. (2012) and to *Monograptus balticus–Pseudomonoclimacis latilobus* condensation surfaces in the open-shelf Mielnik-IG1 section (Kozłowski and Sobień 2012).

Acknowledgments EJ acknowledges the financial support of the Consultation Board for the Student Scientific Movement, University of Warsaw (grants no. 5/III/2010 and 1/III/2011) and of the Deutsche Forschungsgemeinschaft (project no. Mu 2352/3). We are grateful to the Facies Editor M. Tucker and the anonymous reviewer for many constructive suggestions, which helped us to improve an earlier version of the manuscript, and for language corrections to M. Tucker and J. Spicer. We thank R. Nawrot, K. Biernacki and T. Segit for help in fieldwork, S. Skompski, and P. Łuczyński for helpful suggestions, G. Widlicki for preparing thin sections, Z. Remin for sharing part of the isotope measurements, and M. Łoziński for help in performing dumpy leveling. We are also grateful to V. Grytsenko and G. Anfimova (Natural History Museum, Kiev) for providing access to Ukrainian literature on the Silurian of Podolia and to museum collections. This paper is a contribution to the International Geoscience Programme (IGCP) Project 591—The Early to Middle Paleozoic Revolution.

References

Abushik AF, Berger AY, Koren TN, Modzalevskaya TL, Nikiforova OI, Predtechenskij NN (1985) The fourth series of the Silurian System in Podolia. Lethaia 18(2):125–146. doi:10.1111/j.1502-3931.1985.tb00691.x

Aldridge RJ, Jeppsson L, Dorning KJ (1993) Early Silurian oceanic episodes and events. J Geol Soc 150(3):501–513. doi:10.1144/gsjgs.150.3.0501

Alth A (1874) Über die Paleozoischen Gebilde Podoliens und deren Versteinerungen. Abhandlungen der Kaiserlich-Königlichen Geologischen Reichsanstalt VII(1):1–79

Azmy K, Veizer J, Bassett MG, Copper P (1998) Oxygen and carbon isotopic composition of Silurian brachiopods: Implications for coeval seawater and glaciations. Geol Soc Am Bull 110(11):1499–1512. doi:10.1130/0016-7606(1998)110<1499:OACICO>2.3.CO;2

Barrick JE, Kleffner MA, Gibson MA, Peavey FN, Karlsson HR (2010) The mid-Ludfordian Lau Event and carbon isotope excursion (Ludlow, Silurian) in southern Laurentia—preliminary results. Bollettino della Società Paleontologica Italiana 49(1):13–33

Bickert T, Pätzold J, Samtleben C, Munnecke A (1997) Paleoenvironmental changes in the Silurian indicated by stable isotopes in brachiopod shells from Gotland, Sweden. Geochimica et Cosmochimica Acta 61(13):2717–2730. doi:10.1016/S0016-7037(97)00136-1

Calner M (2005a) A Late Silurian extinction event and anachronistic period. Geology 33(4):305–308. doi:10.1130/G21185.1

Calner M (2005b) Silurian carbonate platforms and extinction events—ecosystem changes exemplified from Gotland, Sweden. Facies 51(1–4):584–591

Calner M, Jeppsson L, Munnecke A (2004) The Silurian of Gotland—part I: review of the stratigraphic framework, event stratigraphy, and stable carbon and oxygen isotope development. Erlanger geologische Abhandlungen—Sonderband 5:113–131

Calner M, Kozłowska A, Masiak M, Schmitz B (2006) A shoreline to deep basin correlation chart for the middle Silurian coupled extinction-stable isotopic event. GFF 128:79–84

Calner M, Eriksson ME, Clarkson ENK, Jeppsson L (2008) An atypical intra-platform environment and biota from the Silurian of Gotland, Sweden. GFF 130:79–86

Cherns L (1982) Palaeokarst, tidal erosion surfaces and stromatolites in the Silurian Eke formation of Gotland, Sweden. Sedimentology 29(6):819–833. doi:10.1111/j.1365-3091.1982.tb00086.x

Colombié C, Lécuyer C, Strasser A (2011) Carbon- and oxygen-isotope records of palaeoenvironmental and carbonate production changes in shallow-marine carbonates (Kimmeridgian, Swiss Jura). Geol Mag 148(1):133–153. doi:10.1017/s0016756810000518

Cramer BD, Saltzman MR (2007a) Early Silurian paired $\delta^{13}C_{carb}$ and $\delta^{13}C_{org}$ analyses from the Midcontinent of North America: implications for paleoceanography and paleoclimate. Palaeogeogr Palaeoclimatol Palaeoecol 256(3–4):195–203. doi:http://dx.doi.org/10.1016/j.palaeo.2007.02.032

Cramer BD, Saltzman MR (2007b) Fluctuations in epeiric sea carbonate production during Silurian positive carbon isotope excursions: a review of proposed paleoceanographic models. Palaeogeogr Palaeoclimatol Palaeoecol 245(1–2):37–45. doi:http://dx.doi.org/10.1016/j.palaeo.2006.02.027

Cramer BD, Brett CE, Melchin MJ, Männik P, Kleffner MA, McLaughlin PI, Loydell DK, Munnecke A, Jeppsson L, Corradini C, Brunton FR, Saltzman MR (2011) Revised correlation of Silurian Provincial Series of North America with global and regional chronostratigraphic units and δ13Ccarb chemostratigraphy. Lethaia 44(2):185–202. doi:10.1111/j.1502-3931.2010.00234.x

Dix GR, Patterson RT, Park LE (1999) Marine saline ponds as sedimentary archives of late Holocene climate and sea-level variation along a carbonate platform margin: Lee Stocking Island, Bahamas. Palaeogeogr Palaeoclimatol Palaeoecol 150(3–4):223–246. doi:10.1016/S0031-0182(98)00184-9

Einasto PE, Abushik AF, Kaljo DL, Koren TN, Modzalevskaya TL, Nestor HE (1986) Osobiennosti silurskoho osadkonakoplenija i associacji fauny w kraevych bassejnach Pribaltiki i Podolii. In: Kaljo DL, Klaamann E (eds) Teoria i opyt ekostratigrafii. Valgus, Tallin, pp 65–72

Eriksson MJ, Calner M (2008) A sequence stratigraphical model for the Late Ludfordian (Silurian) of Gotland, Sweden: implications for timing between changes in sea level, palaeoecology, and the global carbon cycle 54(2):253–276

Fanton KC, Holmden C (2007) Sea-level forcing of carbon isotope excursions in epeiric seas: implications for chemostratigraphy. Can J Earth Sci 44(6):807–818. doi:10.1139/e06-122

Freytet P, Verrecchia EP (2002) Lacustrine and palustrine carbonate petrography: an overview. J Paleolimnol 27(2):221–237

Gierlowski-Kordesch E (2010) Lacustrine carbonates. In: Alonso-Zarza AM, Tanner LH (eds) Carbonates in continental settings. Facies, environments and processes. Developments in sedimentology, vol 61. Elsevier, Amsterdam, pp 1–101

Gischler E, Swart PK, Lomando AJ (2009) Stable isotopes of carbon and oxygen in modern sediments of carbonate platforms, barrier reefs, atolls, and ramps: patterns and implications. In: Swart PK, Eberli GP, McKenzie JA (eds) Perspectives in carbonate geology: a tribute to the career of Robert Nathan Ginsburg, vol 41., Int Assoc Sedimentol Spec PublWiley, Oxford, pp 61–74

Harzhauser M, Piller WE, Latal C (2007) Geodynamic impact on the stable isotope signatures in a shallow epicontinental sea. Terra Nova 19(5):324–330. doi:10.1111/j.1365-3121.2007.00755.x

Holmden C, Creaser RA, Muehlenbachs K, Leslie SA, Bergström SM (1998) Isotopic evidence for geochemical decoupling between ancient epeiric seas and bordering oceans: implications for secular curves. Geology 26(6):567–570. doi:10.1130/0091-7613(1998)026<0567:iefgdb>2.3.co;2

Huff WD, Bergström SM, Kolata DR (2000) Silurian K-bentonites of the Dnestr Basin, Podolia, Ukraine. J Geol Soc 157(2):493–504. doi:10.1144/jgs.157.2.493

Immenhauser A, Della Porta G, Kenter JAM, Bahamonde JR (2003) An alternative model for positive shifts in shallow-marine carbonate $\delta^{13}C$ and $\delta^{18}O$. Sedimentology 50(5):953–959. doi:10.1046/j.1365-3091.2003.00590.x

Ishchenko TA (1975) Pozdnesilurijskaja flora Podolii. Naukova Dumka, Kiev

Jeppsson L (1990) An oceanic model for lithological and faunal changes tested on the Silurian record. J Geol Soc 147(4):663–674. doi:10.1144/gsjgs.147.4.0663

Jeppsson L, Aldridge RJ (2000) Ludlow (late Silurian) oceanic episodes and events. J Geol Soc 157(6):1137–1148. doi:10.1144/jgs.157.6.1137

Jeppsson L, Talent JA, Mawson R, Simpson AJ, Andrew AS, Calner M, Whitford DJ, Trotter JA, Sandström O, Caldon H-J (2007) High-resolution Late Silurian correlations between Gotland, Sweden, and the Broken River region, NE Australia: lithologies, conodonts and isotopes. Palaeogeogr Palaeoclimatol Palaeoecol 245(1–2):115–137. doi:10.1016/j.palaeo.2006.02.032

Jeppsson L, Talent JA, Mawson R, Andrew A, Corradini C, Simpson AJ, Wigforss-Lange J, Schönlaub HP (2012) Late Ludfordian correlations and the Lau Event. In: Talent JA (ed) Earth and life. International year of planet earth. Springer, Netherlands, pp 653–675. doi:10.1007/978-90-481-3428-1_21

Kaljo D (1970) Silur Estonii. Valgus, Tallinn

Kaljo D, Martma T (2006) Application of carbon isotope stratigraphy to dating the Baltic Silurian rocks. GFF 128(2):123–129. doi:10.1080/11035890601282123

Kaljo D, Kiipli T, Martma T (1997) Carbon isotope event markers through the Wenlock–Pridoli sequence at Ohesaare (Estonia) and Priekule (Latvia). Palaeogeogr Palaeoclimatol Palaeoecol 132(1–4):211–223. doi:10.1016/S0031-0182(97)00065-5

Kaljo DL, Grytsenko VP, Martma T, Mõtus MA (2007) Three global carbon isotope shifts in the Silurian of Podolia (Ukraine): stratigraphical implications. Estonian J Earth Sci 56(4):205–220

Kaljo D, Martma T, Grytsenko VP, Brazauskas A, Kaminskas D (2012) Přídolí carbon isotope trend and upper Silurian to lowermost Devonian chemostratigraphy based on sections in Podolia (Ukraine) and the East Baltic area. Estonian J Earth Sci 61(3):162–180

Kiipli T, Tsegelnyuk P, Kallaste T (2000) Volcanic interbeds in the Silurian of the southwestern part of the East European Platform. Proc Estonian Acad Sci Geol 49:163–176

Koren' TN, Abushik AF, Modzalevskaya TL, Predtechenskij NN (1989) Podolia. In: Holland CH, Bassett MG (eds) A global standard for the Silurian system. Geological series, vol 9. National Museum of Wales, Cardiff, pp 141–149

Kozłowski W (2003) Age, sedimentary environment and palaeogeographical position of the Late Silurian oolitic beds in the Holy Cross Mountains (Central Poland). Acta Geol Pol 53(4):341–357

Kozłowski W, Munnecke A (2010) Stable carbon isotope development and sea-level changes during the Late Ludlow (Silurian) of the Łysogóry region (Rzepin section, Holy Cross Mountains, Poland). Facies 56(4):615–633

Kozłowski W, Sobień K (2012) Mid-Ludfordian coeval carbon isotope, natural gamma ray and magnetic susceptibility excursions in the Mielnik IG-1 borehole (Eastern Poland)—dustiness as a possible link between global climate and the Silurian carbon isotope record. Palaeogeogr Palaeoclimatol Palaeoecol 339–341:74–97. doi:10.1016/j.palaeo.2012.04.024

Lehnert O, Frýda J, Buggisch W, Munnecke A, Nützel A, Kříž J, Manda S (2007) $\delta^{13}C$ records across the late Silurian Lau event: new data from middle palaeo-latitudes of northern peri-Gondwana (Prague Basin, Czech Republic). Palaeogeogr Palaeoclimatol Palaeoecol 245(1–2):227–244. doi:10.1016/j.palaeo.2006.02.022

Loydell DK, Frýda J (2011) At what stratigraphical level is the mid Ludfordian (Ludlow, Silurian) positive carbon isotope excursion in the type Ludlow area, Shropshire, England? Bull Geosci 86(2):197–208

Małkowski K, Racki G, Drygant D, Szaniawski H (2009) Carbon isotope stratigraphy across the Silurian–Devonian transition in Podolia, Ukraine: evidence for a global biogeochemical perturbation. Geol Mag 146(5):674–689. doi:10.1017/S0016756809006451

Manda Š, Štorch P, Slavík L, Frýda J, Kříž J, Tasáryová Z (2012) The graptolite, conodont and sedimentary record through the late Ludlow Kozlowskii Event (Silurian) in the shale-dominated succession of Bohemia. Geol Mag 149(3):507–531. doi:10.1017/S0016756811000847

Martma T, Brazauskas A, Kaljo D, Kaminskas D, Musteikis P (2005) The Wenlock–Ludlow carbon isotope trend in the Vidukle core, Lithuania, and its relations with oceanic events. Geol Q 49(2):223–234

Melchin MJ, Holmden C (2006) Carbon isotope chemostratigraphy of the Llandovery in Arctic Canada: implications for global correlation and sea-level change. GFF 128:173–180

Munnecke A, Samtleben C, Bickert T (2003) The Ireviken Event in the lower Silurian of Gotland, Sweden—relation to similar Palaeozoic and Proterozoic events. Palaeogeogr Palaeoclimatol Palaeoecol 195(1–2):99–124. doi:http://dx.doi.org/10.1016/S0031-0182(03)00304-3

Munnecke A, Calner M, Harper DAT, Servais T (2010) Ordovician and Silurian sea–water chemistry, sea level, and climate: a synopsis. Palaeogeogr Palaeoclimatol Palaeoecol 296(3–4):389–413. doi:10.1016/j.palaeo.2010.08.001

Nikiforova OI, Predtechenskij NN (1968) A guide to the geological excursion on Silurian and Lower Devonian deposits of Podolia (middle Dnestr River). The Ministry of Geology of the USSR. All-Union Geological Scientific Research Institute (VSEGEI), Leningrad

Nikiforova OI, Predtechenskij NN, Abushik AF, Ignatovich MM, Modzalevskaya TL, Berger AY, Novoselova LS, Burkov YK (1972) Opornyj razrez Silura i Nizhnego Devona Podolii. Nauka, Leningrad

Nikiforova OI, Modzalevskaya TL, Bassett MG (1985) Review of the upper Silurian and lower Devonian articulate brachiopods of Podolia. Special papers in palaeontology, vol 34. The Palaeontological Association, London

Oehlert AM, Lamb-Wozniak KA, Devlin QB, Mackenzie GJ, Reijmer JJG, Swart PK (2012) The stable carbon isotopic composition of organic material in platform derived sediments: implications for reconstructing the global carbon cycle. Sedimentology 59(1):319–335. doi:10.1111/j.1365-3091.2011.01273.x

Paris F, Grahn Y (1996) Chitinozoa of the Silurian-Devonian boundary sections in Podolia, Ukraine. Palaeontology 39(3):629–649

Park LE, Gierlowski-Kordesch EH (2007) Paleozoic lake faunas: establishing aquatic life on land. Palaeogeogr Palaeoclimatol Palaeoecol 249(1–2):160–179. doi:10.1016/j.palaeo.2007.01.008

Saltzman MR (2001) Silurian $\delta^{13}C$ stratigraphy: a view from North America. Geology 29(8):671–674

Samtleben C, Munnecke A, Bickert T (2000) Development of facies and C/O-isotopes in transects through the Ludlow of Gotland: evidence for global and local influences on a shallow-marine environment. Facies 43(1):1–38

Sanz-Montero ME, Rodríguez-Aranda JP, García Del Cura MA (2008) Dolomite–silica stromatolites in Miocene lacustrine deposits from the Duero Basin, Spain: the role of organotemplates in the precipitation of dolomite. Sedimentology 55(4):729–750. doi:10.1111/j.1365-3091.2007.00919.x

Sibley DF, Gregg JM (1987) Classification of dolomite rock textures. J Sediment Res 57(6):967–975. doi:10.1306/212F8CBA-2B24-11D7-8648000102C1865D

Skompski S, Łuczyński P, Drygant DM, Kozłowski W (2008) High-energy sedimentary events in lagoonal successions of the Upper Silurian of Podolia, Ukraine. Facies 54(2):277–296

Swart PK (2008) Global synchronous changes in the carbon isotopic composition of carbonate sediments unrelated to changes in the global carbon cycle. Proc Natl Acad Sci 105(37):13741–13745. doi:10.1073/pnas.0802841105

Swart PK, Eberli G (2005) The nature of the $\delta^{13}C$ of periplatform sediments: Implications for stratigraphy and the global carbon cycle. Sediment Geol 175(1–4):115–129. doi:http://dx.doi.org/10.1016/j.sedgeo.2004.12.029

Teller L (1997) The subsurface Silurian in the East European Platform. Palaeontologia Polonica 56:7–21

Tsegelnyuk P (1980a) Rukshinskaya i tsiganskaya serii (verkhnij silur-nizhnij dewon) Podolii i Volhynii. Preprint Instituta Geologicheskih Nauk AN USSR, Institut Geologicheskih Nauk, Kiev

Tsegelnyuk P (1980b) Yarugskaya i malinovetskaya serii (nizhniy-verkhniy silur) Podolii i Volhynii. Preprint Instituta geologicheskih nauk AN USSR, Institut Geologicheskih Nauk, Kiev

Tsegelnyuk P, Grytsenko VP, Konstantynenko LI, Ishchenko AA, Abushik AF, Bogoyavlenskaya OB, Drygant D, Zayka-Novatskyi WS, Kadlets NM, Kyselev GN, Sytova WA (1983) The Silurian of Podolia, a guide of the excursion. Naukova Dumka, Kiev

Tucker ME (1978) Triassic Lacustrine sediments from South Wales: shore-zone, evaporites and carbonates. In: Matter A, Tucker ME (eds) Modern and ancient Lake Sediments. Blackwell Publishing Ltd., Oxford, pp 205–224

Valero-Garcés BL, Aguilar JG (1992) Shallow carbonate lacustrine facies models in the Permian of the Aragon-Bearn basin (Western Spanish-French Pyrenees). Carbonates Evaporites 7(2):94–107. doi:10.1007/BF03175624

Van Lith Y, Warthmann R, Vasconcelos C, McKenzie JA (2003) Microbial fossilization in carbonate sediments: a result of the bacterial surface involvement in dolomite precipitation. Sedimentology 50(2):237–245. doi:10.1046/j.1365-3091.2003.00550.x

Vannier J, Wang SQ, Coen M (2001) Leperditicopid arthropods (Ordovician-Late Devonian): functional morphology and ecological range. J Paleontol 75(1):75–95

Vasconcelos C, McKenzie JA (1997) Microbial mediation of modern dolomite precipitation and diagenesis under anoxic conditions (Lagoa Vermelha, Rio de Janeiro, Brazil). J Sediment Res 67(3):378–390. doi:10.1306/D4268577-2B26-11D7-8648000102C1865D

Wenzel B, Joachimski MM (1996) Carbon and oxygen isotopic composition of Silurian brachiopods (Gotland/Sweden): palaeoceanographic implications. Palaeogeogr Palaeoclimatol Palaeoecol 122(1–4):143–166. doi:10.1016/0031-0182(95)00094-1

Wenzel B, Lécuyer C, Joachimski MM (2000) Comparing oxygen isotope records of Silurian calcite and phosphate—δ18O compositions of brachiopods and conodonts. Geochim Cosmochim Acta 64(11):1859–1872. doi:10.1016/S0016-7037(00)00337-9

Wigforss-Lange J (1999) Carbon isotope ^{13}C enrichment in Upper Silurian (Whitcliffian) marine calcareous rocks in Scania, Sweden. GFF 121:273–279